FPRINT-93-52

Fermilab Library
0 1160 0025568 1

FPRINT-93-52

Negative $\delta\rho$ in the Standard Model with Four Families and Two Higgs Doublets

delta rho

P. Q. Hung, R. McCoy and D. Singleton

Department of Physics, University of Virginia, Charlottesville, VA 22901

(June 16, 1993)

FERMILAB
JUL 07 1993
LIBRARY

Abstract

We examine consequences of a fourth generation of quarks and leptons within the context of the Standard Model with two Higgs doublets. In particular, we discuss the contribution of heavy vector meson bound states of fourth-generation quarks, formed by the exchange of Higgs bosons, to the ρ parameter. We also include the contribution coming solely from the scalar sector. Our results are parameterized by the amount of global isospin breaking coming from the fermion and scalar sectors. It is found that the way fermions couple to the Higgs doublets crucially determines whether or not one can have a heavy ($\gtrsim$ 150 GeV) top quark and/or a light ($\lesssim$ 80 GeV) charged scalar and/or rare Z decays such as $Z \to \bar{N}\nu_\tau + N\bar{\nu}_\tau$, where N is the fourth-generation neutral lepton.

Typeset using REVTEX

I. INTRODUCTION

The search for the top quark and for the Higgs boson plays a central role in current particle physics research activities. Their discovery or non-discovery will reveal a great deal about the structure of the minimal Standard Model [1] and its possible extensions. By "minimal" we mean three generations of quarks and leptons and one Higgs doublet. In contrast with the gauge boson masses where theoretical predictions (once $sin^2\theta_W$ is measured) are rather impressive, the masses of the fermion and scalar sectors are completely arbitrary. For this reason and in the absence of a plausible theory of fermion and scalar masses, one would like somehow to narrow down the possible mass ranges based on existing experimental data. Such is the goal of [2] , [3] and of the present manuscript.

At this writing, the top quark candidate of 150 GeV at the Central Detector Facility (CDF) is not yet confirmed so we shall assume throughout this paper that its mass is still arbitrary. If, however, the top quark mass is indeed 150 GeV and if it proves difficult to unambiguously confirm its existence at CDF (because of background problems and/or unconventional top decays) then another way to look for it is obviously necessary. We have indicated in [3] how a 150-GeV top quark might give rise to "large" branching ratios for some rare Z decays (explained below) within the context of four generations. This would be an indirect way to detect the top quark in that mass range. The possibility that the top quark is heavier than 150 GeV cannot be dismissed however. Keeping that possibility in mind, we have also examined the theoretical and experimental implications of a very heavy ($\gtrsim$ 150 GeV) top quark within the framework of a four-family and one-Higgs-doublet model. It was found that the maximum top quark mass can be quite high ($\approx$ 360 GeV) depending on the mass and mass-splitting of the fourth generation *and* on the Higgs boson mass. This was allowed because of the contribution from vector-meson bound states of fourth-generation fermions by the Higgs boson exchange to the ρ parameter. Because of this bound-state mechanism, one cannot help but appreciate the intrincate interplay between the Higgs boson mass and various fermion masses such as that of the top quark for example.

An interesting consequence of the model is the existence of characteristic signatures which can be probed by existing accelerators even in the absence of further confirmation of the top quark at CDF. (As stated above, these signatures could also be an indirect way to detect a 150-GeV top quark if it actually has that particular mass.) These are the "monojet" events coming from the following rare Z decays: $Z \to \bar{N}\nu_\tau + N\bar{\nu}_\tau$, where N is the fourth generation neutrino, provided 46 GeV $\lesssim m_N \lesssim$ 85 GeV. The word "monojet" refers to the event in which N decays into a jet and ν_τ escapes undetected. As we have stressed in [3], the observation of such a monojet and its branching ratio would provide quantitative information about the masses and mixing angles of the top quark and the fourth generation fermions, and even the mass of the Higgs boson.

In this paper, we will be examining a scenario in which there are two Higgs doublets and four generations (Scenario III). In particular, we will apply the bound state mechanism of [2] to this scenario. We then compare our results with the one-Higgs doublet and four generations results of [3] (Scenario I) and also with the two-Higgs doublets and three generations model (Scenario II). It turns out that, in many instances, the differences between these three scenarios are quite striking. Also, it turns out that Scenario III can be quite restrictive as far as the way fermions couple to the two Higgs doublets is concerned. Correlations between the top quark mass and various masses of the scalar sector can be quite different for each model considered. We will show that there is a parameter range where one can easily distinguish one model from another. We will restrict ourselves in this paper to non-supersymmetric models.

The plan of the paper is as follows. First we discuss the two-Higgs doublet model, emphasizing in particular the mass spectrum of the scalar sector along with various angles. We then examine the bound state mechanism of [2] applied to the heavy fourth generation in the presence of two Higgs doublets. In this discussion we will examine different schemes of Yukawa coupling between fermions and scalars. Next we will compare the results with those obtained in models with three generations and two Higgs doublets, and four generations and one Higgs doublet. We will show in a series of graphs various allowed regions for the masses

of the scalars and the mass of the top quark. Finally we shall discuss phenomenological implications of various Yukawa coupling schemes showing whether or not one can have a heavy ($\gtrsim$ 150 GeV) top quark and/or a light ($\lesssim$ 80 GeV) charged scalar and or rare Z decays such as $Z \to \bar{N}\nu_\tau + N\bar{\nu}_\tau$, where N is the fourth-generation neutral lepton.

II. THE TWO-HIGGS DOUBLET MODEL

A. The Scalar Sector

The potential at tree level for the two-Higss doublet model is given by [4]

$$\begin{aligned} V(\phi_1,\phi_2) = {} & \lambda_1(\phi_1^\dagger\phi_1 - v_1^2/2)^2 + \lambda_2(\phi_2^\dagger\phi_2 - v_2^2/2)^2 \\ & +\lambda_3[(\phi_1^\dagger\phi_1 - v_1^2/2) - (\phi_2^\dagger\phi_2 - v_2^2/2)]^2 \\ & +\lambda_4[(\phi_1^\dagger\phi_1)(\phi_2^\dagger\phi_2) - (\phi_1^\dagger\phi_2)(\phi_2^\dagger\phi_1)] + \lambda_5(Im\phi_1^\dagger\phi_2)^2 \end{aligned} \tag{1}$$

A discrete symmetry is imposed to arrive at this form of the potential, namely $\phi_1 \to \phi_1$ and $\phi_2 \to -\phi_2$. We are not concerned in this paper of the possibility of CP violation coming from the Higgs sector and, in consequence, we shall set all vacuum expectation values (VEV) to be real for simplicity. They are given by

$$\langle\phi_1\rangle = \begin{pmatrix} 0 \\ \frac{v_1}{\sqrt{2}} \end{pmatrix}, \langle\phi_2\rangle = \begin{pmatrix} 0 \\ \frac{v_2}{\sqrt{2}} \end{pmatrix} \tag{2}$$

The neutral fields are shifted as

$$\sqrt{2}\,\phi_1^0 = h_1 + v_1 + i\phi_1^3 \tag{3a}$$

$$\sqrt{2}\,\phi_2^0 = h_2 + v_2 + i\phi_2^3 \tag{3b}$$

The two physical neutral Higgs bosons are linear combinations of h_1 and h_2. The two neutral Goldstone boson and pseudo-Goldstone boson are linear combinations of ϕ_1^3 and ϕ_2^3. Putting Eq. (3) into Eq. (1) one obtains the mixing matrix in the neutral physical Higgs sector given by

$$2\begin{pmatrix} (\lambda_1+\lambda_3)v_1^2 & -\lambda_3 v_1 v_2 \\ -\lambda_3 v_1 v_2 & (\lambda_2+\lambda_3)v_2^2 \end{pmatrix} \tag{4}$$

The mixing matrix for the charged sector can be read off Eq. (1) and is given by

$$\frac{\lambda_4}{2}\begin{pmatrix} v_1^2 & -v_1 v_2 \\ -v_1 v_2 & v_2^2 \end{pmatrix} \tag{5}$$

Finally the mixing matrix for the Goldstone sector is

$$\frac{\lambda_5}{2}\begin{pmatrix} v_1^2 & -v_1 v_2 \\ -v_1 v_2 & v_2^2 \end{pmatrix} \tag{6}$$

With

$$tan\beta = \frac{v_1}{v_2} \tag{7}$$

the mass eigenstates of Eq. (5) are given by

$$w^{\pm} = cos\beta\ \phi_2^{\pm} + sin\beta\ \phi_1^{\pm} \tag{8a}$$

$$\zeta^{\pm} = -sin\beta\ \phi_2^{\pm} + cos\beta\ \phi_1^{\pm} \tag{8b}$$

The mass eigenvalues for the charged sector are

$$m_{w^{\pm}}^2 = 0 \tag{9a}$$

$$m_{\zeta^{\pm}}^2 = \frac{\lambda_4}{2}(v_1^2 + v_2^2) \tag{9b}$$

The mass eigenstates of Eq. (6) are given by

$$z^0 = cos\beta\ \phi_2^3 + sin\beta\ \phi_1^3 \tag{10a}$$

$$\zeta^0 = -sin\beta\ \phi_2^3 + cos\beta\ \phi_1^3 \tag{10b}$$

and its mass eigenvalues are

$$m_{z^0}^2 = 0 \tag{11a}$$

$$m_{\zeta^0}^2 = \frac{\lambda_5}{2}(v_1^2 + v_2^2) \tag{11b}$$

The massless $w^{\pm}$ and z^0 are absorbed by the gauge fields while $\zeta^{\pm,0}$ are the physical pseudo-Goldstone bosons. As for the physical Higgs scalars, the mass eigenstates of Eq. (4) are given by

$$H_1 = cos\alpha\, h_1 + sin\alpha\, h_2 \tag{12a}$$

$$H_2 = -sin\alpha\, h_1 + cos\alpha\, h_2 \tag{12b}$$

and its mass eigenvalues are

$$m_{H_1}^2 = 2(\lambda_2 + \lambda_3)\, v_2^2\, m_1^2 \tag{13a}$$

$$m_{H_2}^2 = 2(\lambda_2 + \lambda_3)\, v_2^2\, m_2^2 \tag{13b}$$

where $m_{1,2}^2$ and $cos\alpha$ are defined by

$$m_{1,2}^2 = \frac{1 + a \mp \sqrt{(1-a)^2 + 4b^2}}{2} \tag{14a}$$

$$a = (\frac{\lambda_1 + \lambda_3}{\lambda_2 + \lambda_3})\, tan^2\beta \tag{14b}$$

$$b = (\frac{\lambda_3}{\lambda_2 + \lambda_3})\, tan\beta \tag{14c}$$

$$cos\alpha = \frac{1}{\sqrt{1 + [(1 - m_2^2)/b]^2}} \tag{14d}$$

Here we have denoted the lighter of the two Higgs bosons by the subscript 1. The couplings λ_i's are constrained so that all the masses squared are positive. These constraints are

$$\lambda_2 + \lambda_3 > 0,\ \lambda_1\, \lambda_2 > -\lambda_3\, (\lambda_1 + \lambda_2),\ \lambda_{4,5} > 0 \tag{15}$$

B. Global SU(2)

The potential (Eq. (1)) is not chiral $SU(2)\otimes SU(2)$ symmetric when $\lambda_4 \neq \lambda_5$. The reason is simply the following. Let us write ϕ_1 and ϕ_2 as

$$\phi_1 = \frac{1}{\sqrt{2}}\begin{pmatrix} \pi_2 - i\pi_1 \\ \sigma + i\pi_3 \end{pmatrix} \quad \phi_2 = \frac{1}{\sqrt{2}}\begin{pmatrix} \pi_2' - i\pi_1' \\ \sigma' + i\pi_3' \end{pmatrix} \tag{16}$$

The real components of $\phi_{1,2}$ form a vector under global $O(4) \sim SU(2) \otimes SU(2)$, namely $\pi_\mu = (\sigma, \pi_i)$, $\pi_\mu' = (\sigma', \pi_i')$ where $i = 1,2,3$. It is easy to see that there are three $O(4)$-invariant products of ϕ_i's given by

$$\phi_1^\dagger\phi_1 = \frac{1}{2}\pi_\mu\pi_\mu \ , \ \phi_2^\dagger\phi_2 = \frac{1}{2}\pi_\mu'\pi_\mu' \ ,$$
$$\phi_1^\dagger\phi_2 + \phi_2^\dagger\phi_1 = \pi_\mu\pi_\mu' \tag{17}$$

where the sum over repeated indices is implied. An $O(4)$-invariant potential can be constructed out of the above invariants. The potential (1) can be rewritten as follows

$$\begin{aligned} V(\phi_1,\phi_2) = {} & \lambda_1(\phi_1^\dagger\phi_1 - v_1^2/2)^2 + \lambda_2(\phi_2^\dagger\phi_2 - v_2^2/2)^2 \\ & +\lambda_3[(\phi_1^\dagger\phi_1 - v_1^2/2) - (\phi_2^\dagger\phi_2 - v_2^2/2)]^2 \\ & +\lambda_4(\phi_1^\dagger\phi_1)(\phi_2^\dagger\phi_2) - \frac{\lambda_5}{4}[\phi_1^\dagger\phi_2 + \phi_2^\dagger\phi_1]^2 + (\lambda_5 - \lambda_4)(\phi_1^\dagger\phi_2)(\phi_2^\dagger\phi_1) \end{aligned} \tag{18}$$

From Eq. (18) one can see that the potential is $O(4)$-symmetric only when $\lambda_4 = \lambda_5$. This implies the equality of the charged and neutral Pseudo-Goldstone masses. If this is the case then $(\zeta^+, \zeta^0, \zeta^-)$ form a triplet under the residual global SU(2) symmetry of the Higgs potential. It is this residual symmetry which ensures that the electroweak parameter ρ is equal to unity at tree level. If $\lambda_4 = \lambda_5$ so that $m_{\zeta^\pm} = m_{\zeta^0}$ this residual symmetry is unbroken by the pseudoscalar sector. When $\lambda_4 \neq \lambda_5$ the explicit breaking of the residual SU(2) by the pseudoscalar sector will manifest itself in the ρ parameter when radiative corrections are taken into account. The deviation from unity of the ρ parameter coming from the pseudoscalar sector should vanish when the pseudoscalars are degenerate in mass. Another source of deviation comes from the mass splitting within a fermion doublet as we shall discuss subsequently.

C. Scalar-Fermion coupling

In the standard model with just one Higgs doublet, the coupling of fermions to the scalar fields is done in only one way, namely

$$\mathcal{L}_Y = g^u \, \bar{q}_L \, \tilde{\phi} \, u_R + g^d \, \bar{q}_L \, \phi \, d_R + h.c. \tag{19}$$

where

$$q_L \equiv \begin{pmatrix} u_L \\ d_L \end{pmatrix} \tag{20}$$

is a generic quark doublet, and

$$\phi \equiv \begin{pmatrix} \phi^+ \\ \phi^0 \end{pmatrix} \tag{21a}$$

$$\tilde{\phi} = i \, \tau_2 \, \phi^* = \begin{pmatrix} \phi^{0*} \\ -\phi^- \end{pmatrix} \tag{21b}$$

If $g^u = g^d = g_q$ (equal up and down masses), one can rewrite Eq. (19) in an $O(4)$-invariant way as

$$\begin{aligned} \mathcal{L}_Y &= g_q \, (\bar{u}_L \, \bar{d}_L) \begin{pmatrix} \phi^{0*} & \phi^+ \\ -\phi^- & \phi^0 \end{pmatrix} \begin{pmatrix} u_R \\ d_R \end{pmatrix} + h.c. \\ &= g_q \, [\bar{u}_L \, u_R \, \phi^{0*} - \bar{d}_L \, u_R \, \phi^- + \bar{u}_L \, d_R \, \phi^+ + \bar{d}_L \, d_R \, \phi^0] + h.c. \\ &= g_q \, [(\bar{u}_L \, u_R + \bar{d}_L \, d_R) \, \frac{\sigma}{\sqrt{2}} \\ &\quad -i \, (\bar{u}_L \, u_R - \bar{d}_L \, d_R) \, \frac{\phi^3}{\sqrt{2}} - \bar{d}_L \, u_R \, \phi^- + \bar{u}_L \, d_R \, \phi^+] + h.c. \end{aligned} \tag{22}$$

Notice that the last line of Eq. (22) represents an isospin-symmetric coupling of the fermions with the triplet (ϕ_1, ϕ_2, ϕ_3) under the remaining global $SU(2)$. (The third line represents Yukawa coupling between global $SU(2)$ singlets.)

When there are more than one doublet of Higgs scalars, the situation complicates a bit. For instance, in the two-doublet model, do all two Higgs doublets couple to fermions or only

one of them does and the other one does not? It is fair to say that only experiments will be able to answer such a question. In consequence, different scenarios will make specific predictions which can be experimentally tested. There are two scenarios which will be considered in this paper.

1. Model Ia

When both Higgs doublets couple to fermions, it is imperative that one doublet couples to the up sector and the other to the down sector in order to avoid flavour-changing neutral currents [6] . It is fair to say that such a requirement based on "naturalness" might not be a sacred condition. In principle, experimental constraints on flavour-changing neutral currents will restrict the allowed parameter space of a scenario in which one has unrestricted arbitrary couplings between fermions and scalars. It is beyond the scope of this paper to consider such a scenario and we shall postpone such an investigation to a future publication.

Let us choose the case in which the up sector couples to ϕ_1 and the down sector to ϕ_2. The Yukawa Lagrangian will be

$$\mathcal{L}_Y = g^u\, \bar{q}_L\, \tilde{\phi}_1\, u_R + g^d\, \bar{q}_L\, \phi_2\, d_R + h.c. \tag{23}$$

It is instructive to split the above couplings into three parts: fermion-Goldstone boson (longitudinal W) coupling, fermion-Pseudo Goldstone boson coupling, and fermion-physical scalar coupling. Using Eqs. (3,7,8,10, 12), we can write these couplings as

$$\mathcal{L}_{FG} = \frac{\sqrt{2}}{v}\,[-i\,(m_u\,\bar{u}_L\,u_R - m_d\,\bar{d}_L\,d_R)\,\frac{z^0}{\sqrt{2}} - m_u\,\bar{d}_L\,u_R\,w^- + m_d\,\bar{u}_L\,d_R\,w^+] + h.c. \tag{24}$$

for the fermion-Goldstone coupling,

$$\begin{aligned}\mathcal{L}_{FPG} = \frac{\sqrt{2}}{v}\,[&-i\,(m_u\,cot\beta\,\bar{u}_L\,u_R + m_d\,tan\beta\,\bar{d}_L\,d_R)\,\frac{\zeta^0}{\sqrt{2}} \\ &-m_u\,cot\beta\,\bar{d}_L\,u_R\,\zeta^- - m_d\,tan\beta\,\bar{u}_L\,d_R\,\zeta^+] + h.c.\end{aligned} \tag{25}$$

for the fermion-Pseudo Goldstone coupling, and

$$\mathcal{L}_{FS} = \frac{m_u}{v_1}\,[\bar{u}\,u[cos\alpha\,H_1 - sin\alpha\,H_2]] + \frac{m_d}{v_2}[\bar{d}\,d[sin\alpha\,H_1 + cos\alpha\,H_2]] \tag{26}$$

for the fermion-physical scalar coupling. We have used in the above equations the relations $v_1 = v\ sin\beta$ and $v_2 = v\ cos\beta$, where $v = 247$ GeV. Several important remarks are in order. One would first like to know the isospin structure of the above couplings.

When $m_u = m_d$, the isospin breaking from fermion mass splitting should disappear. One then examines to see whether or not any other isospin breaking shows up in the above couplings. First, when $m_u = m_d$, Eq. (24) has the same form as the last line of Eq. (22) which is itself isospin invariant, and it therefore gives no contribution to isospin breaking in that limit. The Goldstone bosons do not break isospin for a degenerate doublet. On the other hand, in the same limit, Eqs. (25) and (26) do not have the isospin-invariant form of Eq. (22) and one would expect isospin breaking to arise from such couplings as we shall see further on. This is the case even if the pseudoscalars were degenerate in mass. For the fermion-physical scalar coupling to be isospin invariant, one would have to have a rather special case, namely $\alpha = \beta = 45°$. So, in general one would expect isospin breaking to appear in this model.

From the above couplings, it is straightforward to derive the appropriate Feynman rules for the computation of various potentials to be used in the bound state problem below.

2. Model Ib

In this model, the up sector is now coupled to ϕ_2 and the down sector to ϕ_1. The Yukawa interaction Lagrangians are simply given by the obvious replacement $\phi_1 \leftrightarrow \phi_2$ in those for Model Ia. The remarks on isospin invariance or breaking are still the same.

3. Model IIa

It might happen that only one Higgs doublet couples to both up and down fermion sectors while both Higgs doublets contribute to the spontaneous breaking of the standard model.

This scenario has interesting consequences. For instance, if the fermion sector couples to ϕ_1 one obtains the following interaction Lagrangians. One has

$$\mathcal{L}_{FG} = \frac{\sqrt{2}}{v}\left[-i\left(m_u\,\bar{u}_L\,u_R - m_d\,\bar{d}_L\,d_R\right)\frac{z^0}{\sqrt{2}} - m_u\,\bar{d}_L\,u_R\,w^- + m_d\,\bar{u}_L\,d_R\,w^+\right] + h.c. \quad (27)$$

for the fermion-Goldstone coupling,

$$\mathcal{L}_{FPG} = \frac{\sqrt{2}cot\beta}{v}\left[-i\left(m_u\,\bar{u}_L\,u_R - m_d\,\bar{d}_L\,d_R\right)\frac{\zeta^0}{\sqrt{2}} - m_u\,\bar{d}_L\,u_R\,\zeta^- + m_d\,\bar{u}_L\,d_R\,\zeta^+\right] + h.c. \quad (28)$$

for the fermion-Pseudo Goldstone coupling, and

$$\mathcal{L}_{FS} = \frac{1}{v_1}\{m_u\,\bar{u}\,u[cos\alpha\,H_1 - sin\alpha\,H_2] + m_d\,\bar{d}\,d[cos\alpha\,H_1 - sin\alpha\,H_2]\} \quad (29)$$

for the fermion-physical scalar coupling. Again, the fermion coupling to the Goldstone bosons, Eq. (27), is the same as in the other cases as one would have expected. In addition, in the case where $m_u = m_d$, all couplings, Eqs. (27, 28, 29), have the isospin-invariant form. In this case, the only source of isospin breaking would come from mass splitting of the pseudoscalars. If the pseudoscalars were also degenerate in mass, Model IIa would give a zero contribution to the ρ parameter as required by isospin invariance. This fact will be used to check our bound state contribution to the ρ parameter.

4. Model IIb

When the fermion sector couples to ϕ_2, one simply makes the obvious replacement $\phi_1 \rightarrow \phi_2$ in the couplings derived for Model IIa. The remarks on isopin invariance are the same.

Before we apply the above scenarios to the computation of vector meson bound states, let us turn our attention to an estimate of the unitarity constraint on the size of the couplings λ's which appear in the Higgs potential. This is important because of the contribution of the scalar sector to $\delta\rho$ through both the vector meson bound states and the one-loop scalar radiative correction.

D. Unitarity Limit

In this section, we shall derive the simplest-minded unitary constraint on some of the couplings in the Higgs potential (1). We shall look only at tree-level unitary constraints coming from the processes $\zeta^+\zeta^- \to \zeta^+\zeta^-$, $w^+w^- \to w^+w^-$, $w^0\,w^0 \to H_{1,2}\,H_{1,2}$, $\zeta^0\,\zeta^0 \to H_{1,2}\,H_{1,2}$. A stricter constraint is obtained by considering extra channels other than the ones mentioned here and by diagonalizing a rather large matrix (for details of this in the one Higgs doublet case see [5]). For our purpose, it might be sufficient to look at these channels since all we really want is to have some idea on the maximal combinations of some of the λ's even in this simple-minded estimate.

The $\zeta^+\zeta^- H_{1,2}$ and $w^+w^- H_{1,2}$ couplings and the ensuing Feyman rules can be read off Eq. (1). They are complicated functions of α, β, and $\lambda_{1,2,3,4}$. We shall denote these (Feynman-rule) couplings by $C_{\zeta H_{1,2}}$ and $C_{wH_{1,2}}$ respectively.

The quartic $\zeta^+\zeta^-$ and w^+w^- couplings give rise to the Feynman rules which will be denoted by $C_{\zeta\zeta}$ and C_{ww} respectively. They will be given explicitely below.

The amplitude for $\zeta^+\zeta^- \to \zeta^+\zeta^-$ is given by

$$\begin{aligned} T_\zeta(s,t) = & -C^2_{\zeta H_1}\,(\frac{m^2_{H_1}}{s-m^2_{H_1}} + \frac{m^2_{H_1}}{t-m^2_{H_1}} + 2) \\ & -C^2_{\zeta H_2}\,(\frac{m^2_{H_2}}{s-m^2_{H_2}} + \frac{m^2_{H_2}}{t-m^2_{H_2}} + 2) \\ & +2\,(C^2_{\zeta H_1} + C^2_{\zeta H_2}) - C^2_{\zeta\zeta} \end{aligned} \tag{30}$$

The amplitude for $w^+w^- \to w^+w^-$ is given by

$$\begin{aligned} T_w(s,t) = & -C^2_{wH_1}\,(\frac{m^2_{H_1}}{s-m^2_{H_1}} + \frac{m^2_{H_1}}{t-m^2_{H_1}} + 2) \\ & -C^2_{wH_2}\,(\frac{m^2_{H_2}}{s-m^2_{H_2}} + \frac{m^2_{H_2}}{t-m^2_{H_2}} + 2) \\ & +2\,(C^2_{wH_1} + C^2_{wH_2}) - C^2_{ww} \end{aligned} \tag{31}$$

The s-wave partial wave amplitude can be computed from

$$a_0 = \frac{1}{32\pi}\int_{-1}^{1} T(s,t)d(cos\theta) \tag{32}$$

One obtains, for $\zeta^+\zeta^- \to \zeta^+\zeta^-$,

$$
\begin{aligned}
a_0^\zeta = & -\frac{C^2_{\zeta H_1}}{32\,\pi}[2 + \frac{m^2_{H_1}}{s - m^2_{H_1}} - \frac{m^2_{H_1}}{s}\ln(1 + \frac{s}{m^2_{H_1}})] \\
& -\frac{C^2_{\zeta H_2}}{32\,\pi}[2 + \frac{m^2_{H_2}}{s - m^2_{H_2}} - \frac{m^2_{H_2}}{s}\ln(1 + \frac{s}{m^2_{H_2}})] \\
& +\frac{1}{16\,\pi}[2(C^2_{\zeta H_1} + C^2_{\zeta H_2}) - C^2_{\zeta\zeta}]
\end{aligned} \tag{33}
$$

For $w^+w^- \to w^+w^-$, one has

$$
\begin{aligned}
a_0^w = & -\frac{C^2_{wH_1}}{32\,\pi}[2 + \frac{m^2_{H_1}}{s - m^2_{H_1}} - \frac{m^2_{H_1}}{s}\ln(1 + \frac{s}{m^2_{H_1}})] \\
& -\frac{C^2_{wH_2}}{32\,\pi}[2 + \frac{m^2_{H_2}}{s - m^2_{H_2}} - \frac{m^2_{H_2}}{s}\ln(1 + \frac{s}{m^2_{H_2}})] \\
& +\frac{1}{16\,\pi}[2(C^2_{wH_1} + C^2_{wH_2}) - C^2_{ww}]
\end{aligned} \tag{34}
$$

In the limit $s \gg m^2_{H_{1,2}}$, the s-wave partial wave amplitudes a_0 tend to $-C^2_{\zeta\zeta,ww}/16\,\pi$. By requiring that $|a_0| \leq 1$, we obtain the condition

$$
4(\lambda_1 + \lambda_3)\,cos^4\beta + 4(\lambda_2 + \lambda_3)\,sin^4\beta - 2\,\lambda_3\,sin^2\beta\,cos^2\beta \leq \sqrt{16\pi} \tag{35}
$$

for $\zeta^+\zeta^- \to \zeta^+\zeta^-$, and

$$
4(\lambda_1 + \lambda_3)\,sin^4\beta + 4(\lambda_2 + \lambda_3)\,cos^4\beta - 2\,\lambda_3\,sin^2\beta\,cos^2\beta \leq \sqrt{16\pi} \tag{36}
$$

for $w^+w^- \to w^+w^-$. In Eq. (35) and Eq. (36), the left-hand sides represent $C_{\zeta\zeta}$ and C_{ww} respectively. They are complicated functions of $m_{H_{1,2}}$ and we shall leave them as such.

The same exercise can be repeated in order to find unitarity constraints on $\lambda_{4,5}$. The channels of interest are $z^0\,z^0 \to H_{1,2}\,H_{1,2}$ and $\zeta^0\,\zeta^0 \to H_{1,2}\,H_{1,2}$. We have

$$
\lambda_5\,cos^2(\alpha + \beta) \leq \sqrt{16\pi} \tag{37}
$$

for $z^0\,z^0 \to H_1\,H_1$ and $\zeta^0\,\zeta^0 \to H_2\,H_2$, and

$$
\lambda_5\,sin^2(\alpha + \beta) \leq \sqrt{16\pi} \tag{38}
$$

for $z^0 z^0 \to H_2 H_2$ and $\zeta^0\zeta^0 \to H_1 H_1$. Using Eq. (11), one can translate the above constraints into those on m_{ζ^0}, namely

$$m_{\zeta^0}^2 \leq \sqrt{4\pi}\, v^2\, Min[\frac{1}{cos^2(\alpha+\beta)}, \frac{1}{sin^2(\alpha+\beta)}] \tag{39}$$

where $v = 247$ GeV and Min refers to the smaller of the two quantities inside the brackets.

For λ_4, we use the following channels to determine its constraint: $w^+ w^- \rightarrow H_{1,2}\, H_{1,2}$ and $\zeta^+ \zeta^- \rightarrow H_{1,2}\, H_{1,2}$. We obtain

$$\lambda_4\, |sin^2\beta\, sin^2\alpha - \frac{1}{4}\, sin2\beta\, sin2\alpha| \leq \sqrt{16\pi} \tag{40}$$

for $w^+ w^- \rightarrow H_1\, H_1$, and

$$\lambda_4\, |sin^2\beta\, cos^2\alpha + \frac{1}{4}\, sin2\beta\, sin2\alpha| \leq \sqrt{16\pi} \tag{41}$$

for $w^+ w^- \rightarrow H_2\, H_2$. We also obtain

$$\lambda_4\, |cos^2\beta\, sin^2\alpha + \frac{1}{4}\, sin2\beta\, cos2\alpha| \leq \sqrt{16\pi} \tag{42}$$

for $\zeta^+ \zeta^- \rightarrow H_1\, H_1$, and

$$\lambda_4\, |cos^2\beta\, cos^2\alpha - \frac{1}{4}\, sin2\beta\, cos2\alpha| \leq \sqrt{16\pi} \tag{43}$$

for $\zeta^+ \zeta^- \rightarrow H_2\, H_2$. Using Eq. (9) the unitarity bound on the charged Higgs mass can now be written as

$$\begin{aligned} m_\pm^2 \leq \sqrt{4\pi}\, v^2\, Min[&\frac{1}{|sin^2\beta\, sin^2\alpha - \frac{1}{4}\, sin2\beta\, sin2\alpha|}, \\ &\frac{1}{|sin^2\beta\, cos^2\alpha + \frac{1}{4}\, sin2\beta\, sin2\alpha|}, \\ &\frac{1}{|cos^2\beta\, sin^2\alpha + \frac{1}{4}\, sin2\beta\, cos2\alpha|}, \\ &\frac{1}{|cos^2\beta\, cos^2\alpha - \frac{1}{4}\, sin2\beta\, cos2\alpha|}] \end{aligned} \tag{44}$$

The conditions (35, 36, 39, 44) will be incorporated into our calculations of the contributions to $\delta\rho$. Even for the scenario where there are only three generations (and two Higgs doublets), the unitarity constraints have to be incorporated for self-consistency. It turns out that they are quite restrictive as we shall see below.

III. BOUND STATE CALCULATION OF $\delta\rho_{NON-PERT}$

In models with arbitrary numbers of Higgs doublets the ρ-parameter (where $\rho = \frac{m_W^2}{m_Z^2 cos^2\theta_W}$ which gives the relative strength of the neutral to charged currents) is unity at tree level due to the "residual" SU(2) symmetry that remains in the Higgs sector after spontaneous symmetry breaking. Radiative corrections and non-perturbative effects can alter this tree level relation to $\rho = 1 + \delta\rho$, where $\delta\rho$ can be generally written by

$$\delta\rho = \left(\frac{\Pi_{+-}(0) - \Pi_{33}(0)}{v^2}\right) \tag{45}$$

$\Pi_{+-}(0)$ and $\Pi_{33}(0)$ are the $W^{\pm}$ and W^0 vacuum polarizations which in principle contain both perturbative and non-perturbative contributions. Previously we have considered the case of a heavy fourth generation of quarks which formed vector meson bound states through the exchange of a Higgs boson. These bound states then mixed with the gauge bosons $W^{\pm}$ and W^0. In analogy with vector-meson-dominace ideas the $V^{\pm,0} - W^{\pm,0}$ mixings are parameterized by

$$\gamma_{V^{\pm,0}-W^{\pm,0}} = i\frac{gm_{V_{\pm,0}}^2}{f_{\pm,0}} \tag{46}$$

Using this mixing parameter and summing up propagators one finds

$$\Pi_{+-}(0) = -\frac{4m_{V+}^2}{f_+^2} \tag{47a}$$

$$\Pi_{33}(0) = -\frac{4m_{V0}^2}{f_0^2} \tag{47b}$$

For more details the reader is referred to reference [2].

In order to determine the contribution of the vector meson bound states to $\delta\rho$ one must obtain $\Pi_{+-}(0)$ and $\Pi_{33}(0)$ of Eqs. (47a , 47b) by solving a bound state problem. Here we will assume that the binding energy is not too large so that we can apply simple nonrelativistic quantum mechanics to the bound state problem. The nonrelativistic potential for any of the four models listed in section II is obtained by writing down the Feynman amplitude for

bound state being considered, and then performing a Fourier transform [7]. In the two gs doublet model the bound state involves not only exchanges of scalar Higgs bosons , H_2), but also exchanges of pseudoscalar Higgs bosons (ζ^0 , $\zeta^\pm$) and Goldstone bosons , $w^\pm$ - the longitudinal W's). In general the nonrelativistic potential can still be written he sum of several Higgs-Yukawa potentials when one considers $^3S_1$ bound states, as we ll show below

$$V(r) = -\sum_{i=1}^{n} \alpha_i \frac{e^{-m_{H_i} r}}{r} \tag{48}$$

viously we have studied the one Higgs doublet case [3] where the bound states were ned solely through the exchange of a single scalar Higgs boson. In the one Higgs doublet del one has to lowest order $\alpha_i = (\frac{m_{f_1} m_{f_2}}{4\pi v^2})$ for a $\bar{f}_1 f_2$ bound state, with $v \approx 250$ GeV. In case with two Higgs doublets the bound state involves not only the exchange of more n one scalar Higgs boson, but of pseudoscalar and charged pseudoscalar bosons as well. rder to take these extra exchanges into account one must carry out the approximation he Feynman amplitudes that are to be Fourier transformed, to order $\mathbf{q}^2$, where $\mathbf{q}$ is momentum of the exchanged Higgs boson. When one considers only $^3S_1$ bound states, the case in this paper, the lowest order term for the Feynman amplitude involving doscalar exchanges contains a factor of $(\frac{\mathbf{q}}{4\mu})^2$ (where $\mu = m_1 m_2/(m_1 + m_2)$ is the ed mass of the system). On Fourier transforming this one finds that the pseudoscalar of the nonrelativistic potential is still of the Yukawa type but reduced by a factor of ^{2} relative to the lowest order term of the scalar exchange. To the same order the scalar nge amplitudes also have a simliar term which is of the opposite sign of the lowest term and so reduces slightly the strength of the scalar coupling.

are interested in the $^3S_1$ bound states since we are looking for mixings with the gauge bosons $W^\pm$ and W^0. Using the Rayleigh-Ritz variational method with a ly normalized trial wave function $u(r) = \frac{1}{r}\chi(r)$ with $\chi(r) = 2\lambda^{3/2} r e^{-\lambda r}$, where λ is a nal parameter, the binding energy as a function of λ can be computed to be ($\hbar = 1$)

$$E_B(\lambda) = \frac{1}{2\mu}\lambda^2 - \sum_{i=1}^{n} \frac{4\lambda^3 \alpha_i}{(m_{H_i} + 2\lambda)^2} \tag{49}$$

Minimizing this with respect to λ ($\frac{dE_B}{d\lambda} = 0$) yields the following equation for λ

$$\sum_{i=1}^{n} \frac{\lambda\alpha_i(3m_{H_i} + 2\lambda)}{(m_{H_i} + 2\lambda)^3} - \frac{1}{4\mu} = 0 \tag{50}$$

λ from Eq. (50) is inserted into Eq. (49), and if E_B is negative then the bound state forms. Next using the formula [9] $|\psi(0)|^2 = \frac{\mu}{2\pi}\langle\frac{dV}{dr}\rangle$ with the potential from Eq. (48) one finds

$$|\psi(0)|^2 = \frac{4\lambda^3\mu}{\pi}\sum_{i=1}^{n} \frac{\alpha_i(m_{H_i} + \lambda)}{(m_{H_i} + 2\lambda)^2} \tag{51}$$

To relate $|\psi(0)|^2$ to the constants $f_{0,\pm}$ from Eqs. (47a , 47b) we assume that the vector meson bound states, $V^{0,\pm}$ exist and compute, for example, the leptonic decays widths $\Gamma(V^0 \to \bar{\nu}\nu)$ and $\Gamma(V^+ \to \bar{e}\nu)$ using the $V^{\pm,0} - W^{\pm,0}$ mixings from Eq. (46) [10]. We find

$$\frac{m_{V^0}^2}{f_0^2} = \frac{3}{4}\frac{(|\psi_0^U(0)|^2 + |\psi_0^D(0)|^2)}{m_{V^0}} \tag{52a}$$

$$\frac{m_{V^+}^2}{f_+^2} = \frac{3}{2}\frac{|\psi_+(0)|^2}{m_{V^+}} \tag{52b}$$

where the right-hand side of Eq. (52a) represents the contributions of the U and D quarks to the neutral vector meson bound state, V^0. Using Eqs. (52a , 52b) , (47b , 47a) and (45) we find

$$\delta\rho_{non-pert} = \frac{6}{v^2}\left[\frac{(|\psi_0^U(0)|^2 + |\psi_0^D(0)|^2)}{2m_{V^0}} - \frac{|\psi_+(0)|^2}{m_{V^+}}\right] \tag{53}$$

In the cases that we considered m_U and m_D were always close to degenerate ($x \equiv \frac{m_D}{m_U} > 0.9$). One reason for this was to ensure that the bound states had time to form. The fastest decay for the fourth generation quarks would come from $U \to D + W$ so if one wants U to be relatively long lived one requires that $m_U \leq m_D + m_W$, or $x \geq 1 - m_W/m_U$, which for a heavy fourth generation translates into the masses of the U and D quarks being nearly degenerate. As a consequence the masses of $V^{\pm,0}$ can be written as $m_{V^+} = m_U + m_D + E_B^+$ and $m_{V^0} = 2m_U + E_B^U$. Using these expressions for the masses of the vector mesons in Eq. (53) we arrive at

$$\delta\rho_{non-pert} = \frac{3}{m_U v^2}\left[\frac{(|\psi_0^U(0)|^2 + |\psi_0^D(0)|^2)}{2 + (E_B^U/m_U)} - \frac{2|\psi_+(0)|^2}{1 + x + (E_B^+/m_U)}\right] \tag{54}$$

This expression for $\delta\rho_{non-pert}$ was evaluated numerically by solving for λ from Eq. (50). This λ was then inserted into Eqs. (51) and (52a, 52b) which was then used to evaluate $\delta\rho_{non-pert}$ in Eq. (53).

A. Model Ia

We now work out the potentials arising from the exchange of the various Higgs bosons for the four cases that were listed in section II. We will work out the first case (up sector coupling to ϕ_1 and down sector coupling to ϕ_2) in some detail and then write down the other cases as they simply involve changing coupling constants.

In the two doublet Higgs model the vector meson bound states involve not only the exchange of neutral scalars between the quarks, but also the exchange of neutral and charged pseudoscalar Higgs bosons. For the charged vector meson, V^+, the Higgs bosons that take part in the binding are H_1, H_2, z^0 and $w^\pm$ (the Goldstone bosons), and ζ^0 and $\zeta^\pm$ (the pseudoGoldstone bosons). Notice that from here on $(w^\pm, z^0)$ refer to the massive longitudinal gauge bosons $(W^\pm, W^0)$. The coupling of the longitudinal gauge bosons, $(W^\pm, W^0)$, to the fermions are identical to those between the corresponding Goldstone bosons and the same fermions. For the neutral vector meson, V^0, only H_1, H_2, ζ^0 and z^0 contribute to the potential. Except for H_1 and H_2, which yield pure scalar potentials, the potentials from the other Higgs bosons are either pure pseudoscalar or a mixture of scalar and pseudoscalar due to the γ_5 in their Feynman rules. For a pure pseudoscalar potentials one obtains, after writing down the Feynman amplitude and Fourier transforming [8]

$$V^{(PS)}(r) = \alpha_i \left(\frac{m_{H_i}}{4\mu}\right)^2 \left[(\sigma^{(1)}\cdot\sigma^{(2)}) + \left(\frac{1}{(m_{H_i}r)^2} + \frac{1}{(m_{H_i}r)} + \frac{1}{3}\right) S_{12}\right] \frac{e^{m_{H_i}r}}{r} \tag{55}$$

where S_{12} is the tensor operator

$$S_{12} = \left[3(\sigma^{(1)}\cdot x)(\sigma^{(2)}\cdot x)/r^2\right] - \sigma^{(1)}\cdot\sigma^{(2)} \tag{56}$$

For the $^3S_1$ state considered here $\langle S_{12}\rangle = 0$ and $\langle\sigma^{(1)}\cdot\sigma^{(2)}\rangle = 1$ so that we get a simple Yukawa potential as in the scalar case except with a reduction factor of $(\frac{m_{H_i}}{4\mu})^2$ out front.

In all cases this factor is less than one since the quarks only start forming bound states of interest with $m_U \geq 300$ GeV and the masses of the Higgs bosons never go much past 600 GeV due to the unitarity constraint that we impose. For the $\bar{U}U$ bound state the pure pseudoscalar part of the potential coming from ζ^0 and z^0 is (using the Feynman rules of section II to determine the form of α_i from Eq. (55))

$$V_{UU}^{(PS)}(r) = \left(\frac{m_{\zeta^0}^2 cos^2\beta}{16\pi v^2 sin^2\beta}\right)\frac{e^{-m_{\zeta^0}r}}{r} + \left(\frac{m_{z^0}^2}{16v^2\pi}\right)\frac{e^{-m_{z^0}r}}{r} \tag{57}$$

where $m_{z^0} = 81$ GeV is the mass of the longitudinal W^0. To obtain the pure pseudoscalar part of the potential for the $\bar{D}D$ bound state $cos\beta$ and $sin\beta$ are exchanged and m_U is replaced with m_D. This pseudoscalar part of the potential is repulsive and does not depend on the mass of the quark since the quark mass from the Feynman rule cancels against that in the reduction factor $(\frac{m_{H_i}}{2m_{U,D}})^2$. Now to the same order in q the Feynman amplitudes for the scalar exchanges are proportional to $-[1 + \frac{q^2}{32\mu^2}]/(q^2 + \mu^2)$. On Fourier transforming this one finds that the general form of the potential coming from the exchange of the scalar Higgs bosons is of the form

$$V^{(S)}(r) = -\alpha_i\left(1 - \frac{m_{H_i}^2}{32\mu^2}\right)\frac{e^{-m_{H_i}r}}{r} \tag{58}$$

The attraction or repulsion of the first term is decreased slightly by the second term. The scalar part of the potential for the $\bar{U}U$ bound state, coming from H_1 and H_2, is given by (again using the Feynman rules from section II)

$$\begin{aligned} V_{UU}^{(S)}(r) = & -\left(\frac{m_U^2 cos^2\alpha}{4\pi v^2 sin^2\beta}\right)\left[1 - \frac{m_{H_1}^2}{8m_U^2}\right]\frac{e^{-m_{H_1}r}}{r} \\ & -\left(\frac{m_U^2 sin^2\alpha}{4\pi v^2 sin^2\beta}\right)\left[1 - \frac{m_{H_2}^2}{8m_U^2}\right]\frac{e^{-m_{H_2}r}}{r} \end{aligned} \tag{59}$$

To obtain the scalar part of the potential of the $\bar{D}D$ bound state for this model simply switch $sin\beta$ and $cos\beta$, and replace m_U with m_D. For the charged vector meson, V^+, in addition to the neutral Higgs bosons contributing to the potential, the charged bosons, $\zeta^\pm$ and $w^\pm$ contribute as well. The couplings of these charged Higgs bosons to the quarks is a mixture between scalar and pseudoscalar coupling which raises the possiblity that the cross terms

could contribute to the potential. However explicit calculations show that the cross terms are 0, therefore the potential from the charged Higgs bosons is just the sum of the potential due to the scalar part and that due to the pseudoscalar part. The potential coming from $\zeta^{\pm}$ is

$$V_{UD}^{(\zeta^{\pm})}(r) = \frac{1}{2\pi v^2}\left(A_1^2\left[1-\frac{m_{\zeta^+}^2}{32\mu^2}\right]+B_1^2\left[\frac{m_{\zeta^+}^2}{16\mu^2}\right]\right)\frac{e^{-m_{\zeta^+}r}}{r} \tag{60}$$

where $A_1 = m_U cot\beta + m_D tan\beta$ and $B_1 = m_U cot\beta - m_D tan\beta$. The first term is the scalar part of the potential while the second term is the pseudoscalar part. The part of the $\bar{U}D$ potential coming from the longitudinal $W^{\pm}$ ($w^{\pm}$) is similar to the potential from Eq. (60). Since $m_{w^+} = m_{z^0}$ the terms of the $\bar{U}D$ potential coming from the Goldstone bosons can be combined into one term with the same overall Yukawa factor, $e^{m_{z^0}r}/r$. Combining the results from Eqs. (55 - 60) one arrives at the following expressions for the potentials, $V_{UU}(r)$, $V_{DD}(r)$, and $V_{UD}(r)$ due the the exchange of all the Higgs bosons

$$\begin{aligned} V_{UU}(r) = & -\left(\frac{m_U^2 cos^2\alpha}{4\pi v^2 sin^2\beta}\right)\left[1-\frac{m_{H_1}^2}{8m_U^2}\right]\frac{e^{-m_{H_1}r}}{r} \\ & -\left(\frac{m_U^2 sin^2\alpha}{4\pi v^2 sin^2\beta}\right)\left[1-\frac{m_{H_2}^2}{8m_U^2}\right]\frac{e^{-m_{H_2}r}}{r} \\ & +\left(\frac{m_{\zeta^0}^2 cot^2\beta}{16\pi v^2}\right)\frac{e^{-m_{\zeta^0}r}}{r}+\left(\frac{m_{z^0}^2}{16v^2\pi}\right)\frac{e^{-m_{z^0}r}}{r} \end{aligned} \tag{61a}$$

$$\begin{aligned} V_{DD}(r) = & -\left(\frac{m_D^2 sin^2\alpha}{4\pi v^2 cos^2\beta}\right)\left[1-\frac{m_{H_1}^2}{8m_D^2}\right]\frac{e^{-m_{H_1}r}}{r} \\ & -\left(\frac{m_D^2 cos^2\alpha}{4\pi v^2 cos^2\beta}\right)\left[1-\frac{m_{H_2}^2}{8m_D^2}\right]\frac{e^{-m_{H_2}r}}{r} \\ & +\left(\frac{m_{\zeta^0}^2 tan^2(\beta)}{16\pi v^2}\right)\frac{e^{-m_{\zeta^0}r}}{r}+\left(\frac{m_{z^0}^2}{16v^2\pi}\right)\frac{e^{-m_{z^0}r}}{r} \end{aligned} \tag{61b}$$

$$\begin{aligned} V_{UD}(r) = & -\left(\frac{m_U m_D sin2\alpha}{4\pi v^2 sin2\beta}\right)\left[1-\frac{m_{H_1}^2}{32\mu^2}\right]\frac{e^{-m_{H_1}r}}{r} \\ & +\left(\frac{m_U m_D sin2\alpha}{4\pi v^2 sin2\beta}\right)\left[1-\frac{m_{H_2}^2}{32\mu^2}\right]\frac{e^{-m_{H_2}r}}{r} \\ & +\frac{1}{2\pi v^2}\left(A_1^2\left[1-\frac{m_{\zeta^+}^2}{32\mu^2}\right]+B_1^2\left[\frac{m_{\zeta^+}^2}{16\mu^2}\right]\right)\frac{e^{-m_{\zeta^+}r}}{r} \end{aligned}$$

$$+\left(\frac{m_{\zeta^0}^2 m_U m_D}{64\pi v^2\mu^2}\right)\frac{e^{-m_{\zeta^0}r}}{r}$$
$$+\frac{1}{4\pi v^2}\left(\frac{C^2}{2}+\frac{D^2 m_{z^0}^2}{64\mu^2}\right)\frac{e^{-m_{z^0}r}}{r} \tag{61c}$$

where $A_1 = m_U cot\beta + m_D tan\beta$, $B_1 = m_U cot\beta - m_D tan\beta$, $C = m_U - m_D$, and $D = m_U + m_D$. The dominant terms in the potentials are those involving the pure scalar Higgs bosons, H_1 and H_2. In the $\bar{U}D$ potential the H_1 part is attractive while the H_2 part is repulsive, unlike the $\bar{U}U$ and $\bar{D}D$ case where both are attractive. This results in the $\bar{U}D$ bound state being weaker in general, and giving a smaller contribution to $\delta\rho_{non-pert}$ from Eq. (53). This leads one to suspect that negative values of $\delta\rho_{non-pert}$ might not exist in this model, and on doing the numerical calculation this is indeed found to be the case. We now simply write down the potentials for the other three models as nothing new is involved except using the different Feynman rules to calculate the various couplings.

B. Model Ib

In the case the couplings of model Ia are reversed - the up sector is coupled to ϕ_2 and the down sector is coupled to ϕ_1. This model is a complement to the first model giving the same values for $\delta\rho_{non-pert}$, but for different parameter ranges.

$$V_{UU}(r) = -\left(\frac{m_U^2 sin^2\alpha}{4\pi v^2 cos^2(\beta)}\right)\left[1-\frac{m_{H_1}^2}{8m_U^2}\right]\frac{e^{-m_{H_1}r}}{r}$$
$$-\left(\frac{m_U^2 cos^2\alpha}{4\pi v^2 cos^2\beta}\right)\left[1-\frac{m_{H_2}^2}{8m_U^2}\right]\frac{e^{-m_{H_2}r}}{r}$$
$$+\left(\frac{m_{\zeta^0}^2 tan^2\beta}{16\pi v^2}\right)\frac{e^{-m_{\zeta^0}r}}{r}+\left(\frac{m_{z^0}^2}{16v^2\pi}\right)\frac{e^{-m_{z^0}r}}{r} \tag{62a}$$

$$V_{DD}(r) = -\left(\frac{m_D^2 cos^2\alpha}{4\pi v^2 sin^2(\beta)}\right)\left[1-\frac{m_{H_1}^2}{8m_D^2}\right]\frac{e^{-m_{H_1}r}}{r}$$
$$-\left(\frac{m_D^2 sin^2\alpha}{4\pi v^2 sin^2\beta}\right)\left[1-\frac{m_{H_2}^2}{8m_D^2}\right]\frac{e^{-m_{H_2}r}}{r}$$
$$+\left(\frac{m_{\zeta^0}^2 cot^2\beta}{16\pi v^2}\right)\frac{e^{-m_{\zeta^0}r}}{r}+\left(\frac{m_{z^0}^2}{16v^2\pi}\right)\frac{e^{-m_{z^0}r}}{r} \tag{62b}$$

$$
\begin{aligned}
V_{UD}(r) = & -\left(\frac{m_U m_D sin2\alpha}{4\pi v^2 sin2\beta}\right)\left[1-\frac{m_{H_1}^2}{32\mu^2}\right]\frac{e^{-m_{H_1}r}}{r} \\
& +\left(\frac{m_U m_D sin2\alpha}{4\pi v^2 sin2\beta}\right)\left[1-\frac{m_{H_2}^2}{32\mu^2}\right]\frac{e^{-m_{H_2}r}}{r} \\
& +\frac{1}{2\pi v^2}\left(A_2^2\left[1-\frac{m_{\zeta^+}^2}{32\mu^2}\right]+B_2^2\left[\frac{m_{\zeta^+}^2}{16\mu^2}\right]\right)\frac{e^{-m_{\zeta^+}r}}{r} \\
& +\left(\frac{m_{\zeta^0}^2 m_U m_D}{64\pi v^2\mu^2}\right)\frac{e^{-m_{\zeta^0}r}}{r} \\
& +\frac{1}{4\pi v^2}\left(\frac{C^2}{2}+\frac{D^2 m_{z^0}^2}{64\mu^2}\right)\frac{e^{-m_{z^0}r}}{r}
\end{aligned}
\tag{62c}
$$

where $A_2 = m_U tan\beta + m_D cot\beta$, $B_2 = m_U tan\beta - m_D cot\beta$, $C = m_U - m_D$, and $D = m_U + m_D$. As in the first model the binding of the $\bar{U}D$ vector meson is weakened due to the opposite signs of the H_1 and H_2 part of the potential. On carrying through the explicit calculation one again finds that there are no negative values for $\delta\rho_{non-pert}$. Both models Ia and Ib violate the "residual" isospin symmetry through the fact that the up and down quark sectors are coupled to different Higgs doublets. Thus even for $x = 1$ and $m_{\zeta^0} = m_{\zeta^\pm}$ $\delta\rho_{non-pert}$ can be non-zero.

C. Model IIa

In this case both the up and down sector quarks couple to ϕ_1.

$$
\begin{aligned}
V_{UU}(r) = & -\left(\frac{m_U^2 cos^2\alpha}{4\pi v^2 sin^2\beta}\right)\left[1-\frac{m_{H_1}^2}{8m_U^2}\right]\frac{e^{-m_{H_1}r}}{r} \\
& -\left(\frac{m_U^2 sin^2\alpha}{4\pi v^2 sin^2\beta}\right)\left[1-\frac{m_{H_2}^2}{8m_U^2}\right]\frac{e^{-m_{H_2}r}}{r} \\
& +\left(\frac{m_{\zeta^0}^2 cot^2\beta}{16\pi v^2}\right)\frac{e^{-m_{\zeta^0}r}}{r}+\left(\frac{m_{z^0}^2}{16v^2\pi}\right)\frac{e^{-m_{z^0}r}}{r}
\end{aligned}
\tag{63a}
$$

$$
\begin{aligned}
V_{DD}(r) = & -\left(\frac{m_D^2 cos^2\alpha}{4\pi v^2 sin^2\beta}\right)\left[1-\frac{m_{H_1}^2}{8m_D^2}\right]\frac{e^{-m_{H_1}r}}{r} \\
& -\left(\frac{m_D^2 sin^2\alpha}{4\pi v^2 sin^2\beta}\right)\left[1-\frac{m_{H_2}^2}{8m_D^2}\right]\frac{e^{-m_{H_2}r}}{r} \\
& +\left(\frac{m_{\zeta^0}^2 cot^2\beta}{16\pi v^2}\right)\frac{e^{-m_{\zeta^0}r}}{r}+\left(\frac{m_{z^0}^2}{16v^2\pi}\right)\frac{e^{-m_{z^0}r}}{r}
\end{aligned}
\tag{63b}
$$

$$
\begin{aligned}
V_{UD}(r) = & -\left(\frac{m_U m_D cos^2\alpha}{4\pi v^2 sin^2\beta}\right)\left[1-\frac{m_{H_1}^2}{32\mu^2}\right]\frac{e^{-m_{H_1}r}}{r} \\
& -\left(\frac{m_U m_D sin^2\alpha}{4\pi v^2 sin^2\beta}\right)\left[1-\frac{m_{H_2}^2}{32\mu^2}\right]\frac{e^{-m_{H_2}r}}{r} \\
& +\frac{cot^2\beta}{4\pi v^2}\left(\frac{C^2}{2}\left[1-\frac{m_{\varsigma^+}^2}{32\mu^2}\right]+D^2\left[\frac{m_{\varsigma^+}^2}{32\mu^2}\right]\right)\frac{e^{m_{\varsigma^+}r}}{r} \\
& +\left(\frac{cot^2\beta m_{\varsigma^0}^2 m_U m_D}{64\pi v^2\mu^2}\right)\frac{e^{-m_{\varsigma^0}r}}{r} \\
& +\frac{1}{4\pi v^2}\left(\frac{C^2}{2}+\frac{D^2 m_{z^0}^2}{64\mu^2}\right)\frac{e^{-m_{z^0}r}}{r}
\end{aligned}
\tag{63c}
$$

where $C = m_U - m_D$ and $D = m_U + m_D$. In this model the signs of the H_1 and H_2 parts of the $\bar{U}D$ potential are the same making the $\bar{U}D$ bound state stronger than in the first two models. This opens up the possibility that one could get negative $\delta\rho_{non-pert}$ as in the one Higgs doublet scenario. The two models where both quark sectors bind to only one of the Higgs doublets are qualitatively similiar to the one Higgs doublet case. On carrying through the calculations we do find negative $\delta\rho_{non-pert}$. The absolute value of these negatives is slightly larger than in the one Higgs model and occurs for much lower values of the quark masses. We shall find in this case that when $x = 1$ and $m_{\varsigma^\pm} = m_{\varsigma^0}$, $\delta\rho_{non-pert} = 0$ identically because of the residual SU(2) symmetry mentioned earlier.

D. Model IIb

In the final model both the up and down sector are coupled to the ϕ_2 Higgs doublet. This model is the complement of model IIa. It gives the same basic values for $\delta\rho_{non-pert}$, but in different ranges of the parameters.

$$
\begin{aligned}
V_{UU}(r) = & -\left(\frac{m_U^2 sin^2\alpha}{4\pi v^2 cos^2\beta}\right)\left[1-\frac{m_{H_1}^2}{8m_U^2}\right]\frac{e^{-m_{H_1}r}}{r} \\
& -\left(\frac{m_U^2 cos^2\alpha}{4\pi v^2 cos^2\beta}\right)\left[1-\frac{m_{H_2}^2}{8m_U^2}\right]\frac{e^{-m_{H_2}r}}{r} \\
& +\left(\frac{m_{\varsigma^0}^2 tan^2\beta}{16\pi v^2}\right)\frac{e^{-m_{\varsigma^0}r}}{r}+\left(\frac{m_{z^0}^2}{16v^2\pi}\right)\frac{e^{-m_{z^0}r}}{r}
\end{aligned}
\tag{64a}
$$

$$
V_{DD}(r) = -\left(\frac{m_D^2 sin^2\alpha}{4\pi v^2 cos^2\beta}\right)\left[1-\frac{m_{H_1}^2}{8m_D^2}\right]\frac{e^{-m_{H_1}r}}{r}
$$

$$
\begin{aligned}
&- \left(\frac{m_D^2 cos^2\alpha}{4\pi v^2 cos^2\beta}\right)\left[1-\frac{m_{H_2}^2}{8m_D^2}\right]\frac{e^{-m_{H_2}r}}{r} \\
&+ \left(\frac{m_{\varsigma^0}^2 tan^2\beta}{16\pi v^2}\right)\frac{e^{-m_{\varsigma^0}r}}{r} + \left(\frac{m_{z^0}^2}{16v^2\pi}\right)\frac{e^{-m_{z^0}r}}{r}
\end{aligned} \tag{64b}
$$

$$
\begin{aligned}
V_{UD}(r) = &- \left(\frac{m_U m_D sin^2\alpha}{4\pi v^2 cos^2\beta}\right)\left[1-\frac{m_{H_1}^2}{32\mu^2}\right]\frac{e^{-m_{H_1}r}}{r} \\
&- \left(\frac{m_U m_D cos^2\alpha}{4\pi v^2 cos^2\beta}\right)\left[1-\frac{m_{H_2}^2}{32\mu^2}\right]\frac{e^{-m_{H_2}r}}{r} \\
&+ \frac{tan^2\beta}{2\pi v^2}\left(\frac{C^2}{2}\left[1-\frac{m_{\varsigma^+}^2}{32\mu^2}\right] + D^2\left[\frac{m_{\varsigma^+}^2}{64\mu^2}\right]\right)\frac{e^{-m_{\varsigma^+}r}}{r} \\
&+ \left(\frac{tan^2\beta m_{\varsigma^0}^2 m_U m_D}{64\pi v^2\mu^2}\right)\frac{e^{-m_{\varsigma^0}r}}{r} \\
&+ \frac{1}{4\pi v^2}\left(\frac{C^2}{2} + \frac{D^2 m_{z^0}^2}{64\mu^2}\right)\frac{e^{-m_{z^0}r}}{r}
\end{aligned} \tag{64c}
$$

where $C = m_U - m_D$ and $D = m_U + m_D$. Again on doing the calculations of $\delta\rho_{non-pert}$ one finds negative values at values of the quark masses which are lower than in the one Higgs doublet case. In both models IIa and IIb $\delta\rho_{non-pert} = 0$ when $x = 1$ and $m_{\varsigma^0} = m_{\varsigma^\pm}$. This is because both quark sectors couple to the same Higgs doublet.

IV. IMPLICATIONS FOR DIFFERENT SCENARIOS AND MODELS

As noted previously, a principal purpose of this paper, in conjunction with our earlier work [2] , [3], is to use the experimental limits upon $\delta\rho$ to differentiate between the usual three generation, one Higgs Standard Model and certain minimal extensions involving a fourth fermion generation and/or a second Higgs doublet. The possible experimental signals that would suggest the minimal Standard Model may have to be modified include the failure to detect the top quark at CDF (i.e., $m_t \gtrsim 150$ GeV), the experimental detection (at LEP II) of a charged or light neutral scalar particle, and finally flavor-changing Z decays which can occur at higher than expected rates due to the presence of a heavy fourth fermion generation. All the various possible rare Z decays - $Z \to \bar{N}\nu_\tau + N\bar{\nu}_\tau$ (for $m_N < m_E$), $Z \to \bar{E}\tau + E\bar{\tau}$ (for $m_N > m_E$), and $Z \to \bar{b}s + b\bar{s}$ - were discussed fully in [3]. Here we will focus on the

"monojet" rare Z decay ($Z \to \bar{N}\nu_\tau + N\bar{\nu}_\tau$) since it gives the most distinctive signal. The ν_τ - neutrino will escape the detector while the N - neutrino will decay mainly into $\tau^- + X$, where X can be $\tau^+\nu_\tau$, $\mu^+\nu_\mu$, $e^+\nu_e$, $\bar{u}d$, $\bar{c}s$. The signal would be a "monojet" containing at least one τ - lepton. The quantity of interest in this rare Z decay is the branching ratio, $BR(Z \to \bar{N}\nu_\tau + N\bar{\nu}_\tau)$ which using the results of [11] is given by

$$\frac{\Gamma(Z \to \bar{N}\nu_\tau + N\bar{\nu}_\tau)}{\Gamma(Z \to \bar{\nu}_\tau\nu_\tau)} = 2\left(\frac{\alpha}{\pi}\right)^2 |I_E(s_0, r)|^2 |V_{E\nu_\tau}|^2 \phi_{N\nu_\tau} \tag{65a}$$

where $V_{E_{\nu_\tau}}$ is the KM mixing angle between the fourth generation charged lepton E and ν_τ, $\phi_{N\nu_\tau}$ is the phase space factor given by

$$\phi_{N\nu_\tau} = \{1 - r_N\}\left\{1 - \frac{1}{2}r_N(1 + r_N)\right\}, \quad r_N \equiv \frac{m_N^2}{M_W^2} \tag{65b}$$

and $I_E(s_0, r_E)$, the vertex factor with $s_0 \equiv \frac{M_Z^2}{M_W^2}$ and $r_E \equiv \frac{M_E^2}{M_W^2}$, given by (for large r_E),

$$\begin{aligned} I_E(s_0, r_E) = &\left(\frac{1}{8sin^2\theta_W}\right) \\ &\times \{r_E + 2.88lnr_E - 6.716 - i1.484 \\ &+ (8.368lnr_E - 3.408)/r_E \\ &+ (9.126lnr_E + 2.26)/r_E^2 \\ &+ (4.043lnr_E + 7.41)/r_E^3 + \ldots\} \end{aligned} \tag{65c}$$

Where $BR(Z \to \bar{\nu}_\tau\nu_\tau) = 0.0666$. This branching ratio increases as the mass (m_E) of the fourth generation, charged lepton inside the loop increases. The branching ratio decreases as the mass of the fourth generation neutrino (m_N) increases, and as the KM mixing ($V_{E\nu_\tau}$) between E and ν_τ decreases. Here we will only consider $|V_{E\nu_\tau}| \simeq \lambda^2 \simeq (0.22)^2$ and $m_N = 46$ GeV in order to obtain the maximum *possible* effect. A more detailed analysis of this and the other flavor-changing Z decays was carried out in [3].

The observation of any of these three experimental signals would indicate that an extension of the minimal Standard Model was needed. Beyond simply indicating that an extension is necessary would one be able to tell what *kind* of extension was called for ? When paired with the current narrow experimental limits upon $\delta\rho$, i.e., $-0.0026 \lesssim \delta\rho \lesssim 0.0056$ [12], such

signals could provide information helping to differentiate the Scenarios mentioned earlier: Scenario I (one Higgs, four generations); Scenario II (two Higgs, three generations); and Scenario III (two Higgs, four generations). The most striking distinction that we find is between the two different models of Scenario III. In Model I (the "normal" coupling case where one Higgs doublet couples to the up fermion sector and the other doublet couples to the down sector) the $\bar{U}D$ bound states form very weakly due to the competing effects of the m_{H_1} and m_{H_2} parts of the potential (see Eq. (61c) and Eq. (62c)). This leads to $\delta\rho$ being strictly positive for the whole range of parameters to which our bound state model applies. These positive values are always larger than the experimental upper limit on $\delta\rho$ (see Table II) so that this model is probably precluded within the parameter range to which our analysis applies. Model II (the "anomalous" coupling case where one Higgs doublet couples to both fermion sectors, while the other Higgs doublet is essentially decoupled from the fermions) however can form strong $\bar{U}D$ bound states since there the m_{H_1} and m_{H_2} parts of the potential were both attractive (see Eq. (63c) and Eq. (64c)). This allows $\delta\rho$ to be negative (see Table III) and allows such distinctive features as a heavier than expected m_t and/or rare Z decays especially the "monojet" decay $Z \to \bar{N}\nu_\tau + N\bar{\nu}_\tau$.

Because our analysis requires the comparison of our theoretical calculation of $\delta\rho$ to the experimental limits it was confined to regions in parameter space where each component of the total $\delta\rho$ could be calculated consistently under our assumptions. In particular, the following constraints were imposed: (i) unitarity limits were imposed upon scalar and pseudoscalar masses, (ii) the parameters (including especially fermion and scalar masses) were such that all bound state calculations were well-approximated by our nonrelativistic model, (iii) no bound-state fermion could decay by the emission of a real W boson (giving bound states time to form), (iv) where relevant, fourth generation fermions either formed bound states or could be treated perturbatively (since our model has no way of calculating nonperturbative contributions from non-bound state fermion loops), and (v) the top quark mass was sufficiently light to permit perturbative treatment of third-generation contributions to $\delta\rho$ (since the top will clearly decay via emission of a real W, making our bound state anal-

ysis inapplicable under assumption (iii) above). In particular, the imposition of unitarity constraints placed significant limits upon the scenarios considered here, as discussed below. Last, our analysis, as illustrated by various figures, concentrates on the relationship between the magnitude of $\delta\rho_{non-pert}$ and the breaking of the residual SU(2) symmetry in the fermion (parameterized by $x = \frac{m_D}{m_U}$) and scalar sectors (parameterized by $y = \frac{m_{\zeta^\pm}}{m_{\zeta^0}}$).

It should be noted that, as a matter of convention and without loss of generality, m_{H_1} was taken to be less than m_{H_2}.

A. $\delta\rho$ In Two-Higgs Doublet Models (Scenario II)

Section III sets forth a procedure for calculating the nonperturbative bound state contribution to $\delta\rho$, under certain assumptions, in scenarios which include a heavy fourth generation of fermions and a two-doublet Higgs sector. However, this is not the only contribution to $\delta\rho$ in such scenarios; $\delta\rho$ will also receive significant perturbative contributions from scalar and third-generation fermion radiative loop diagrams. In Scenario II (three generations two Higgs doublets) these radiative corrections are the only contributions to $\delta\rho$, while Scenario III (four generations two Higgs doublets) also have the non-pertubative, fourth generation bound state part.

The radiative third-generation fermion contributions were discussed in [13] and the scalar-gauge contribution was calculated in [14] . The results are

$$\delta\rho_{3-pert} = \left(\frac{3}{8\pi^2 v^2}\right) f(m_b^2, m_t^2) \tag{66a}$$

$$\begin{aligned}\delta\rho_{SG} = \left(\frac{1}{4\pi v}\right)^2 & [sin^2\alpha(f(m_{H_1}^2, m_{\zeta^+}^2) + f(m_{\zeta^0}^2, m_{\zeta^+}^2) - f(m_{H_1}^2, m_{\zeta^0}^2)) \\ & +cos^2\alpha(f(m_{H_2}^2, m_{\zeta^+}^2) + f(m_{\zeta^0}^2, m_{\zeta^+}^2) - f(m_{H_2}^2, m_{\zeta^0}^2))]\end{aligned} \tag{66b}$$

where

$$f(m_1^2, m_2^2) = \frac{m_1^2 + m_2^2}{2} - \frac{m_1^2 m_2^2}{m_1^2 - m_2^2} ln \frac{m_1^2}{m_2^2} \tag{67}$$

$\delta\rho_{3-pert}$ is always positive while, in certain regions, the scalar-gauge contribution can be negative. Taking unitarity constraints into account, the scalar-gauge contribution can reach a minimum value of $\delta\rho \approx -0.009$, sufficient to accommodate a top quark mass of up to approximately 215 GeV (assuming no other factors make additional positive contributions to $\delta\rho$). The importance of unitarity can be seen by the fact that without the unitarity constraint $\delta\rho_{SG}$ could be as low as $\simeq -0.017$. This would allow a top quark mass of up to 270 GeV. The principal mechanism by which unitarity constrains $\delta\rho$ is through the placing of maximum values upon the Higgs sector masses, particularly m_{H_2}, large values of which seem to be crucial for obtaining the minimum values of $\delta\rho_{SG}$. Table I gives a sampling of some points which we will discuss.

The first six points in Table I show values of $\delta\rho_{SG}$ that were representative of the smallest values that we found using our unitarity constraints. There were two general factors that contributed to large negative $\delta\rho_{SG}$. The first was the splitting between m_{H_1} and m_{H_2}. The second was the splitting between m_{ζ^0} and $m_{\zeta^\pm}$. Large splittings in these masses gave large negative $\delta\rho_{SG}$. Without the unitarity constraints, particularly on m_{H_2}, we obtained negatives on the order of -0.017 rather than our result of $\delta\rho_{SG} \approx$ -0.009. The splitting between m_{ζ^0} and $m_{\zeta^\pm}$ was a measure of how much the residual SU(2) symmetry of the Higgs potential (Eq. (18)) was broken. For $m_{\zeta^0} = m_{\zeta^\pm}$ ($\lambda_4 = \lambda_5$) this SU(2) symmetry remained unbroken and so $\delta\rho_{SG} = 0$ regardless of the values of the other parameters. Viewing $\delta\rho$, from any source, (perturbative or non-perturbative) as a measure of how much the residual symmetry of the Higgs potential was broken gave a powerful check on our calculations. Setting the sources of symmetry breaking in the Lagranian equal to zero required that $\delta\rho = 0$ (this does not hold for Scenario III Model I since there one source of the SU(2) symmetry breaking was the result of *how* the Higgs sector was coupled to the fermions as discussed below). The next three points in Table I show how reducing the mass splittings increase the value of $\delta\rho_{SG}$. The most negative $\delta\rho$ of these points ≈ -0.0037 only increases the value of a possible heavy top to $m_t \approx 175$ GeV. The last six points in Table I illustrate points with negative $\delta\rho_{SG}$ and a charged Higgs scalar in the range detectable at LEP II, $m_{\zeta^\pm} \leq 80$ GeV. These

negatives are very small and would allow the top quark to be only marginally heavier than the current bounds based on the minimal Standard Model with three generations and one Higgs doublet.

Scenario II would allow a heavy top up to roughly $m_t \approx 215$ GeV. From Table I one can see that with such a heavy top the only Higgs sector particles which might be accessible at the next generation of particle accelerators would be m_{H_1} and the pseudoscalar m_{ζ^0}. If one wanted a charged scalar which was detectable at LEP II, Scenario II would contribute only a very small negative $\delta\rho_{SG}$ and would not significantly affect the current bounds on m_t.

B. Scenario III, Model I

Scenario III involves four generations and two Higgs doublets, and Model I is the usual case in two-Higgs doublet models, where one doublet couples to the up fermion sector while the other doublet couples to the down sector ("normal coupling"). In all Scenario III models, $\delta\rho$ has three components:

$$\delta\rho_{tot} = \delta\rho_{SG} + \delta\rho_{3-pert} + \delta\rho_{4-nonpert}, \tag{68}$$

where $\delta\rho_{3-pert}$ represents the perturbative fermion loop contributions from the top quark and $\delta\rho_{4-nonpert}$ represents the bound state contribution from the fourth generation of fermions. Assuming a top quark mass of at least 100 GeV or so, the experimental limits upon $\delta\rho_{tot}$ require that $\delta\rho_{SG} + \delta\rho_{4-nonpert} \lesssim .0025$.

Table II gives as sampling of points which were calculated in this model (All the points are for the coupling of Model Ia. The other coupling scheme gives basically the same results but at complementary angles α and β). All the $\delta\rho$'s are positive and far exceed the experimental limit. This was the case throughout the range of parameters for which our bound state model was valid. The reason for this lies in the $\bar{U}D$ potentials of Eqs. (61c , 62c). In both these potentials the m_{H_2} part of the potential (as well as all the other contribuitions except for m_{H_1}) is repulsive which leads to the $\bar{U}D$ bound state being extremely weak when it forms

at all. From Eq. (53) one can see that in order to get a negative $\delta\rho$ from the bound state one must have a large contribution from the $\bar{U}D$ state. In this model one can never get a strong $\bar{U}D$ bound state.

One unique feature of this model, as compared to the other models considered in this paper, is that in addition to the breaking of the global isospin symmetry from the mass splitting between m_{ζ^0} and $m_{\zeta^\pm}$, and between m_D and m_U there is another source of symmetry breaking coming from the fact that the Higgs doublets, ϕ_1 and ϕ_2, couple to different fermion sectors. Thus even when $m_{\zeta^0} = m_{\zeta^\pm}$ and $m_U = m_D$, $\delta\rho = 0$ is not required unless one has the special case where $\alpha = \beta = 45°$.

In short, within the framework of our bound state model our calculations indicate Scenario III Model I (four generations, two Higgs, "normal" coupling to the fermions) is most probably ruled out. However, the principal effect of our model is to provide a mechanism for negative bound state contributions to $\delta\rho$ from a fourth fermion generation that otherwise would generally be forbidden, or at least very narrowly constrained, by the experimental limits upon $\delta\rho$. In Scenario III Model I, our methods cannot produce such negative contributions, and thus we cannot provide a justification for believing that Scenario III Model I is permitted under the current experimental limits on $\delta\rho$.

C. Scenario III, Model II

Scenario III Model II involves four fermion generations and two Higgs doublets, where both up and down fermion sectors couple to the same Higgs doublet, and the other Higgs doublet is essentially decoupled from the fermion sector. In many respects this scenario is similar to Scenario I (four generations, one Higgs doublet), but the presence of two Higgs doublets contributing to spontaneous symmetry breaking permits smaller vacuum expectation values for the scalar particles and thus, from Eq. (53), raises the possibility of larger negative contributions to $\delta\rho$ and bound state formation for lighter fermions than was obtained in Scenario I.

Model II does result in possible negative contributions to $\delta\rho$ across a broad region of parameter space as can be seen from Table III. The reason that negative $\delta\rho$ could occur in this model while they were absent in the previous model can be found, again, by looking at the form of the $\bar{U}D$ potentials in the two cases Eq. (63c , 64c). Here both the m_{H_1} and m_{H_2} parts of the potential are attractive allowing for much stronger $\bar{U}D$ bound states. The two models in this section (Models IIa and IIb) are actually more similar to the case of Scenario I than to the preceding model. The difference between the present case and Scenario I lies in the complications brought about by the dependence on the angles α and β. In Scenario I negative $\delta\rho$ only occured for $m_U \gtrsim 600$ GeV, and the most negative value we obtained was $\delta\rho_{max} \approx$ -0.03. In the present case one might suspect that a much larger negative value of $\delta\rho$ is possible since the VEV in Eq. (53) can be smaller than in the one Higgs doublet case. Table III bears out this suspicion with negative $\delta\rho$ that are up to two times the maximum value from the one Higgs case. A second difference that can be seen from Table III is that the m_U 's for which substantial negatives occur are much lower than in the 1 Higgs case. In the mass range 250 GeV $< m_U <$ 1000 GeV our model gave negative $\delta\rho$ for a large range of the other parameters. Outside of this mass range our assumptions started the break down. In particular at the upper limit, $m_U = 1000$ GeV, our nonrelativistic assumption was suspect, and making m_U lower than 250 GeV leads to problems with treating m_t perturbatively.

One of the most fruitful ways of looking at this complicated model is to take $\delta\rho$ as a measure of the breaking of the residual SU(2) isospin symmetry. In this model where one Higgs doublet binds to both the up and down fermion sectors there are two sources of isospin breaking : the mass splitting between m_U and m_D (which we parameterize by $x = \frac{m_D}{m_U}$) and the mass splitting between m_{ζ^0} and $m_{\zeta^\pm}$ (which we parameterize by $y = \frac{m_{\zeta^\pm}}{m_{\zeta^0}}$). This is in contrast with the "normal" coupling model of the previous section where there was an additional isospin breaking due to the up and down fermion sectors coupling to different Higgs doublets. Also by setting x =1 and y =1 we had a powerful check on our complicated and involved bound state calculations since then it was required that $\delta\rho = 0$ regardless of the other parameters. Figs. (1-9) give a good summary of some of the main

features of this model, bringing together information about the bound state contribution to $\delta\rho$, the experimental limits on $\delta\rho$, and the rare Z decay $Z \to \bar{N}\nu_\tau + N\bar{\nu}_\tau$. Figs. (1-3) show the point $m_U = 500$ GeV, $m_{H_1} = 200$ GeV, $m_{H_2} = 310$ GeV, $m_{\zeta^0} = 145$ GeV, $\alpha = 38°$, and $\beta = 30°$, for $m_t = 150$, 200 , and 250 GeV respectively. The Figures show curves of constant $\delta\rho$ as a function of the two isospin breaking parameters x and y. The upper curve represents the upper experimental limit of $0.0056 \geq \delta\rho$ under the assumption that the branching ratio for $Z \to \bar{N}\nu_\tau + N\bar{\nu}_\tau$ is just big enough to be marginally detected with the production of 10^8 Z's (by marginally detectable we mean that $BR(Z \to \bar{N}\nu_\tau + N\bar{\nu}_\tau) \geq 10^{-8}$). The branching ratio was calculated using Eqs. (65a , 65b , 65c). In Figs. (1-9), in order to show the maximum possible results for the rare Z decay, we took $m_N = 46$ GeV and $|V_{E\nu_\tau}| = (0.22)^2$. Increasing m_N and/or decreasing $|V_{E\nu_\tau}|$ shrinks the region between the dashed and solid striping (this is called the "allowed" region in Figs. (1-9)) without yielding anything qualitatively different. Under these assumptions the upper curve corresponds to the charged fourth generation lepton, E, having a mass of $m_E = 175$ GeV. The dashed region above the curve, while not a strictly forbidden region, represents the range of x and y for which $\delta\rho$ is not negative enough to allow an observable rare Z decay. The lower curve in the figures comes from one of two sources. Under one limit m_E (and therefore $BR(Z \to \bar{N}\nu_\tau + N\bar{\nu}_\tau)$) is restricted from becoming larger due to the requirement that the lepton sector's contribution to $\delta\rho$ can be calculated from the perturbative formula Eq. (66a). The other limit on the lower curve comes from making m_E large enough so that $Z \to \bar{N}\nu_\tau + N\bar{\nu}_\tau$ would have already been seen. For the values of m_N and $|V_{E\nu_\tau}|$ that we assume this corresponds to $BR(Z \to \bar{N}\nu_\tau + N\bar{\nu}_\tau) \approx 10^{-6}$ and to a charged lepton mass of $m_E \approx 575$ GeV. In Figs. (1-6) the lower curve comes from the first limit. For the point $m_U = 500$ GeV in Figs. (1-3) the value of m_E was required to be less than 400 GeV in order to make the use of the pertubative formula Eq. (66a) valid; for the point $m_U = 600$ GeV in Figs. (4-6) m_E had be be below 500 GeV. The other parameters in these figures were picked in order so as to give sizeable negative $\delta\rho$ and yet still allow m_E to become large enough to have a detectable branching ratio for the rare Z decay. In Figs. (7-9) the lower curve

represents the limit where the rare Z decays would have been observed already rather than the failure of the pertubative formula for m_E. In all these $x - y$ graphs a dot-dashed line has been drawn at the limit of where LEP II would be able to detect the charged scalar $\zeta^{\pm}$.

Finally Figs. (10-12) show the behaviour of $\delta\rho$ as a function of the angle β for the parameter points from Figs. (1-9). This helps show that the negative $\delta\rho$ are not the result of some specially picked values for the angles.

V. CONCLUSION

The analysis we have given above for Scenarios II and III along with our previous analysis of Scenario I (four fermion generations and one Higgs doublet) [3] allows for a heavy top ($m_t > 150$ GeV), and/or light charged or neutral scalars, and/or rare Z decays of the type discussed, with only small extensions to the minimal Standard Model. While at present there is no experimental reason for prefering one scenario over the other, we have tried to outline signals that would be observable at future accelerators that would give a hint as to which model is more viable. All the extensions we considered can have negative values for $\delta\rho$, and therefore they can all relax the present upper limit on m_t. Scenario II, taking into account the unitarity constraints on the scalar masses, can have a top mass of up to $m_t \approx$ 215 GeV. Scenarios I and III (Model II) both allow $\delta\rho$ to become more negative and therefore m_t to become larger and/or rare "monojet" Z-decays to become observable. In Scenario I one could get a top mass of up to $m_t \approx 350$ GeV. Table III indicates that in Scenario III Model II one could get even larger top masses, one must be careful, since here bound states formed at much lower fermion masses which could for some values of the parameters make an $m_t = 400$ GeV, for example, non-pertubative. Thus if the top were found to be larger than 215 GeV Scenario II would probably be in difficulties. While Scenario II does not have rare Z decays of the type discussed here, it does have the possiblity of detectable, light charged scalars ($\zeta^{\pm}$) and/or pseudoscalars (ζ^0) which would distinguish it from Scenario I. However from Table I one can see that for the charged scalar to be in the range detectable

at LEP II ($m_{\zeta^\pm} \leq 80$ GeV) the negative $\delta\rho$ is small. Scenario III Model I seems to be ruled out in the region to which our analysis applies, but Scenario III Model II seems to allow many interesting results (heavy m_t, rare, "monojet" Z decays, light charged scalars and/or pseudoscalars) for a wide range of parameters. The "monojet" Z decays are the best way to differentiate between Scenario II and Scenario's I and III. The main distinguishing feature between Scenario III Model II and Scenario I are the presence, in the former case, of charged scalars and pseudoscalars, a detection of which would clearly favour Scenario III Model II. Another difference, as pointed out above, is that in Scenario III the bound states can form at much lower masses for the fourth generation quarks (m_U and m_D) leading to a better chance of directly observing them if a fourth generation exists. Finally it should be pointed out that there are regions of the parameters for which there would not be any direct way of distinguishing between the proposed extensions. If for example $m_t \approx 200$ GeV, but no charged scalars or pseudoscalars were detected, and no rare Z decays were observed, (up to the limits of the accelerator being used) then one would need to extend the minimal Standard Model, but all of the three scenarios considered here would be equally viable. However within the framework of our bound state model we have tried to give a thorough list of *possible* events which would help pick out one case over the others.

This work was supported in part by the U.S. Department of Energy under Grant No. DE-A505-89ER40518.

REFERENCES

[1] S.L. Glashow, Nucl. Phys. **22**, 579 (1961) ; S. Weinberg, Phys. Rev. Lett. **19**, 1264 (1967) ; A. Salam, in *Elementary Particle Theory: Relativistic Groups and Analiticity* (Nobel Symposium No. 8) edited by N. Svartholm (Almquist and Wiksell, Stockholm, 1968), p. 367

[2] P.Q. Hung, Phys. Rev. Lett. **69**, 3143 (1992)

[3] P.Q. Hung, R. McCoy, D. Singleton, University of Virginia report (1992)

[4] P.Q. Hung and H.B. Thacker, Phys. Rev. **D31**, 2866 (1985)

[5] B.W. Lee, C. Quigg, H.B. Thacker, Phys. Rev. **D16**, 1519 (1977)

[6] S. Glashow and S. Weinberg, Phys. Rev. **D15**, 1958 (1977)

[7] J.J. Sakurai, *Advanced Quantum Mechanics* (Addison-Wesley Publishing Company, 1982), p. 259

[8] J.J. Sakurai, *Advanced Quantum Mechanics* (Addison-Wesley Publishing Company, 1982), p. 265

[9] C. Quigg and J. Rosner, Phys. Rep. **C56**, 167 (1979)

[10] C. Quigg, *Gauge Theories of the Strong, Weak, and Electromagnetic Interactions* (Addison-Wesley Publishing Company, 1983), p. 21 problem 1.8

[11] J. Bernabéu, A. Pich, A. Santamaría, Phys. Lett. **200B**, 569 (1988)

[12] G. Altarelli, Invited talk at the 27th Rencontre de Moriond (1992), edited by J. Tran Thanh Van (Editions Frontières)

[13] M.B. Einhorn, D.R.T. Jones, and M. Veltman, Nucl. Phys. **B191**, 146 (1981), and references therein

[14] C.D. Froggatt, R.G. Moorhouse and I.G. Knowles, Phys. Rev. **D45** 2471 (1992)

FIGURES

FIG. 1. The "allowed" region in the $x(=\frac{m_D}{m_U})$ - $y(=\frac{m_{\zeta^\pm}}{m_{\zeta^0}})$ plane for $m_t = 150$ GeV and with $m_U = 500$ GeV, $m_{H_1} = 200$ GeV, $m_{H_2} = 310$ GeV, $m_{\zeta^0} = 145$ GeV, $\alpha = 38°$, and $\beta = 30°$. The area below the dotdashed line is the experimentally accessible region for detecting a charged scalar Higgs at LEP II.

FIG. 2. The "allowed" region in the $x(=\frac{m_D}{m_U})$ - $y(=\frac{m_{\zeta^\pm}}{m_{\zeta^0}})$ plane for $m_t = 200$ GeV and with $m_U = 500$ GeV, $m_{H_1} = 200$ GeV, $m_{H_2} = 310$ GeV, $m_{\zeta^0} = 145$ GeV, $\alpha = 38°$, and $\beta = 30°$. The area below the dotdashed line is the experimentally accessible region for detecting a charged scalar Higgs at LEP II.

FIG. 3. The "allowed" region in the $x(=\frac{m_D}{m_U})$ - $y(=\frac{m_{\zeta^\pm}}{m_{\zeta^0}})$ plane for $m_t = 250$ GeV and with $m_U = 500$ GeV, $m_{H_1} = 200$ GeV, $m_{H_2} = 310$ GeV, $m_{\zeta^0} = 145$ GeV, $\alpha = 38°$, and $\beta = 30°$. The area below the dotdashed line is the experimentally accessible region for detecting a charged scalar Higgs at LEP II.

FIG. 4. The "allowed" region in the $x(=\frac{m_D}{m_U})$ - $y(=\frac{m_{\zeta^\pm}}{m_{\zeta^0}})$ plane for $m_t = 150$ GeV and with $m_U = 600$ GeV, $m_{H_1} = 250$ GeV, $m_{H_2} = 295$ GeV, $m_{\zeta^0} = 175$ GeV, $\alpha = 34°$, and $\beta = 40°$. The area below the dotdashed line is the experimentally accessible region for detecting a charged scalar Higgs at LEP II.

FIG. 5. The "allowed" region in the $x(=\frac{m_D}{m_U})$ - $y(=\frac{m_{\zeta^\pm}}{m_{\zeta^0}})$ plane for $m_t = 200$ GeV and with $m_U = 600$ GeV, $m_{H_1} = 250$ GeV, $m_{H_2} = 295$ GeV, $m_{\zeta^0} = 175$ GeV, $\alpha = 34°$, and $\beta = 40°$. The area below the dotdashed line is the experimentally accessible region for detecting a charged scalar Higgs at LEP II.

FIG. 6. The "allowed" region in the $x(=\frac{m_D}{m_U})$ - $y(=\frac{m_{\zeta^\pm}}{m_{\zeta^0}})$ plane for $m_t = 250$ GeV and with $m_U = 600$ GeV, $m_{H_1} = 250$ GeV, $m_{H_2} = 295$ GeV, $m_{\zeta^0} = 175$ GeV, $\alpha = 34°$, and $\beta = 40°$. The area below the dotdashed line is the experimentally accessible region for detecting a charged scalar Higgs at LEP II.

FIG. 7. The "allowed" region in the $x(=\frac{m_D}{m_U})$ - $y(=\frac{m_{\zeta^\pm}}{m_{\zeta^0}})$ plane for $m_t = 150$ GeV and with $m_U = 700$ GeV, $m_{H_1} = 300$ GeV, $m_{H_2} = 415$ GeV, $m_{\zeta^0} = 190$ GeV, $\alpha = 30°$, and $\beta = 46°$. The area below the dotdashed line is the experimentally accessible region for detecting a charged scalar Higgs at LEP II.

FIG. 8. The "allowed" region in the $x(=\frac{m_D}{m_U})$ - $y(=\frac{m_{\zeta^\pm}}{m_{\zeta^0}})$ plane for $m_t = 200$ GeV and with $m_U = 700$ GeV, $m_{H_1} = 300$ GeV, $m_{H_2} = 415$ GeV, $m_{\zeta^0} = 190$ GeV, $\alpha = 30°$, and $\beta = 46°$. The area below the dotdashed line is the experimentally accessible region for detecting a charged scalar Higgs at LEP II.

FIG. 9. The "allowed" region in the $x(=\frac{m_D}{m_U})$ - $y(=\frac{m_{\zeta^\pm}}{m_{\zeta^0}})$ plane for $m_t = 250$ GeV and with $m_U = 700$ GeV, $m_{H_1} = 300$ GeV, $m_{H_2} = 415$ GeV, $m_{\zeta^0} = 190$ GeV, $\alpha = 30°$, and $\beta = 46°$. The area below the dotdashed line is the experimentally accessible region for detecting a charged scalar Higgs at LEP II.

FIG. 10. The variation of $\delta\rho$ as a function of β for $m_U = 500$ GeV, $m_{H_1} = 200$ GeV, $m_{H_2} = 310$ GeV, $m_{\zeta^0} = 145$ GeV, $m_{\zeta^\pm} = 132$ GeV, $\alpha = 38°$, and $x = 0.99$.

FIG. 11. The variation of $\delta\rho$ as a function of β for $m_U = 600$ GeV, $m_{H_1} = 250$ GeV, $m_{H_2} = 295$ GeV, $m_{\zeta^0} = 175$ GeV, $m_{\zeta^\pm} = 150$ GeV, $\alpha = 34°$, and $x = 0.98$.

FIG. 12. The variation of $\delta\rho$ as a function of β for $m_U = 700$ GeV, $m_{H_1} = 300$ GeV, $m_{H_2} = 415$ GeV, $m_{\zeta^0} = 190$ GeV, $m_{\zeta^\pm} = 160$ GeV, $\alpha = 30°$, and $x = 0.985$.

TABLES

TABLE I. Sample of points with negative $\delta\rho_{SG}$

m_{H_1}	m_{H_2}	m_{ζ^0}	$m_{\zeta^\pm}$	α	β	$\delta\rho_{SG}$
50	661	15	330	4	45	-0.00949
85	678	25	340	11	45	-0.00933
120	658	30	400	6	45	-0.00928
155	663	50	375	10	45	-0.00902
160	668	40	360	11	45	-0.00915
130	672	20	365	12	45	-0.00922
50	103	330	260	10	10	-0.00139
50	144	505	380	23	10	-0.00379
50	76	365	170	7	10	-0.00210
85	665	15	80	7	45	-0.00206
120	659	15	80	5	45	-0.00207
155	662	15	80	9	45	-0.00205
50	77	470	80	10	10	-0.00014
50	79	375	80	39	25	-0.00034
50	66	400	80	2	45	-0.00043

TABLE II. Sample of points for Scenario III Model I (4 generations 2 Higgs doublets with the "up" and "down" fermion sectors coupled to different doublets). All $\delta\rho$'s in this scenario where positive and larger than the experimental upper bound of 0.0056 for the parameter range to which our model applied

m_U	m_{H_1}	m_{H_2}	m_{ζ^0}	$m_{\zeta^\pm}$	x	α	β	$\delta\rho$
400	30	568	15	575	0.91	38	50	0.0141
400	30	482	20	560	0.90	40	50	0.0169
400	30	513	25	525	0.87	41	50	0.0131
400	30	457	40	580	0.89	43	52	0.0206
400	30	423	30	530	0.86	44	50	0.0174
425	30	602	85	625	0.85	45	48	0.0207
425	40	490	15	575	0.91	41	50	0.0187
425	40	578	20	575	0.91	44	50	0.0170
425	40	459	40	620	0.91	44	50	0.0264
425	35	564	35	610	0.91	45	50	0.0230
450	40	467	15	625	0.83	44	50	0.0266
450	40	459	30	630	0.83	44	50	0.0273
450	40	564	20	635	0.83	45	50	0.0243
450	40	578	85	625	0.83	44	50	0.0211
450	40	493	40	640	0.84	45	50	0.0274

TABLE III. Sample of points for Scenario III Model II (both "up" and "down" sectors couple to the same Higgs doublet) Large negative values of $\delta\rho$ were obtained for this model.

m_U	m_{H_1}	m_{H_2}	m_{ζ^0}	$m_{\zeta^\pm}$	x	α	β	$\delta\rho$
300	50	312	182	60	0.95	10	20	-0.0375
300	50	312	142	60	0.95	10	20	-0.0221
300	50	312	102	60	0.95	10	20	-0.0087
400	65	282	216	75	0.92	36	25	-0.0520
400	65	282	216	75	0.91	36	25	-0.0442
400	65	282	216	75	0.90	36	25	-0.0362
500	115	384	196	122	0.97	40	30	-0.0628
500	115	384	196	122	0.97	40	35	-0.0160
500	115	384	196	122	0.97	40	40	-0.0030
600	160	211	178	67	0.96	25	40	-0.0423
600	160	211	178	67	0.96	35	40	-0.0418
600	160	211	178	67	0.96	45	40	-0.0411
700	215	505	276	93	0.96	44	50	-0.0337
700	215	455	276	93	0.96	44	50	-0.0379
700	215	405	276	93	0.96	44	50	-0.0423
800	125	337	165	52	0.98	30	60	-0.0193
800	175	337	165	52	0.98	30	60	-0.0183
800	225	337	165	52	0.98	30	60	-0.0172

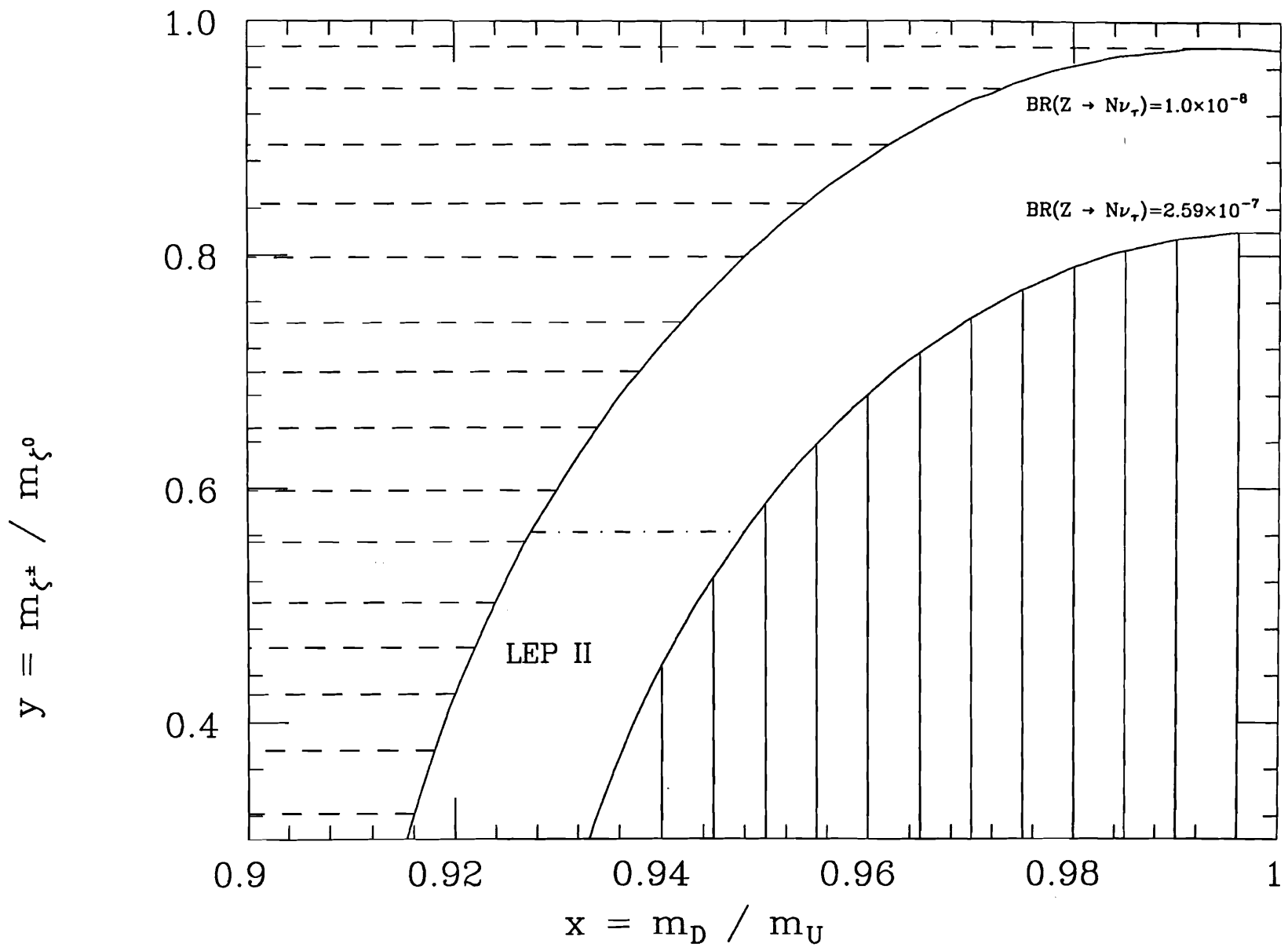
1.0
0.8
0.6
0.4
0.9
0.92
0.94
0.96
0.98
1
$x = m_D / m_U$
$y = m_{\zeta^\pm} / m_{\zeta^0}$
$BR(Z \to N\nu_\tau)=1.0\times10^{-8}$
$BR(Z \to N\nu_\tau)=2.59\times10^{-7}$
LEP II

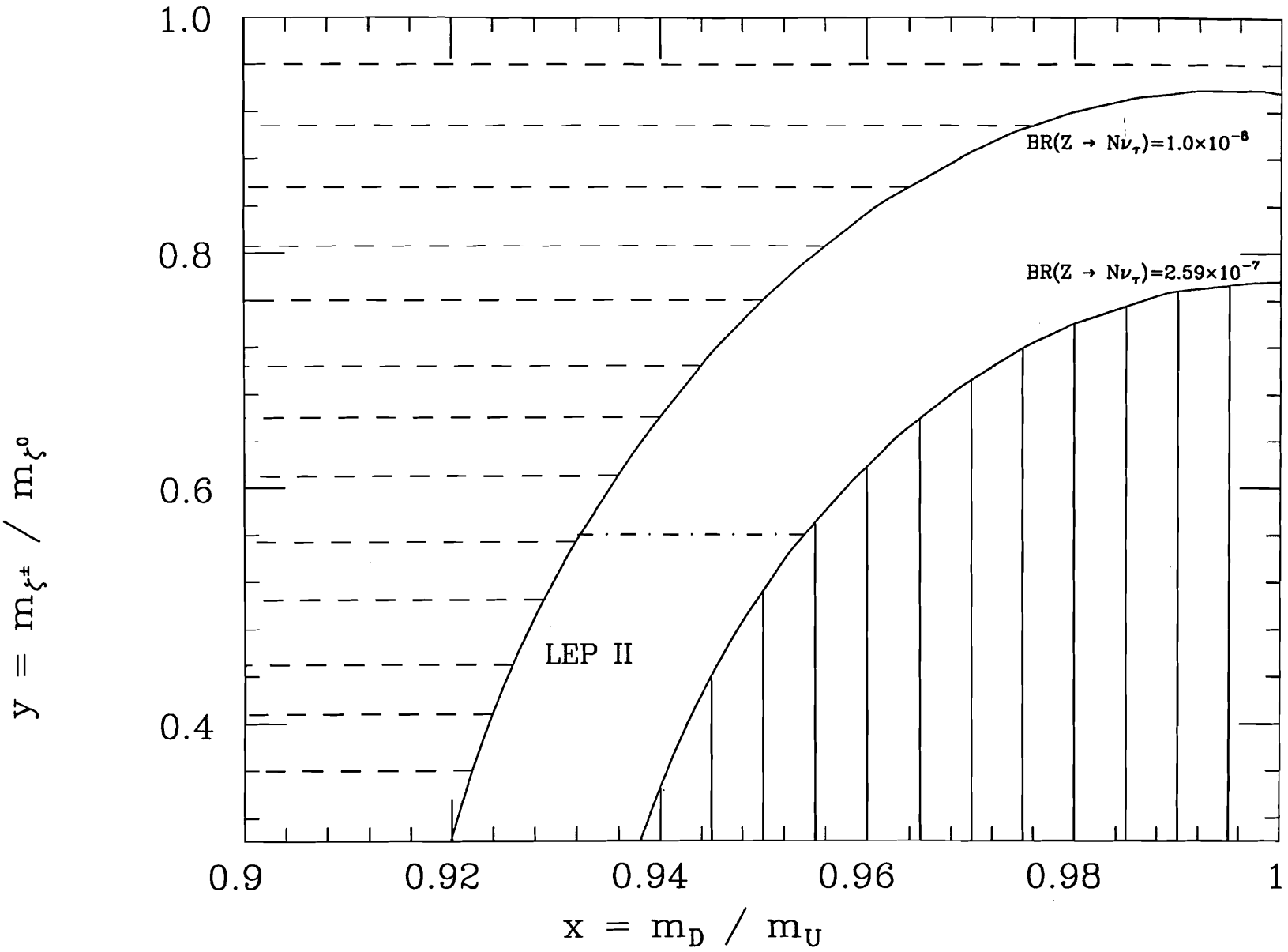
1.0
0.8
0.6
0.4
0.9
0.92
0.94
0.96
0.98
1
$y = m_{\zeta^\pm} / m_{\zeta^0}$
$x = m_D / m_U$
$BR(Z \to N\nu_\tau)=1.0\times10^{-8}$
$BR(Z \to N\nu_\tau)=2.59\times10^{-7}$
LEP II

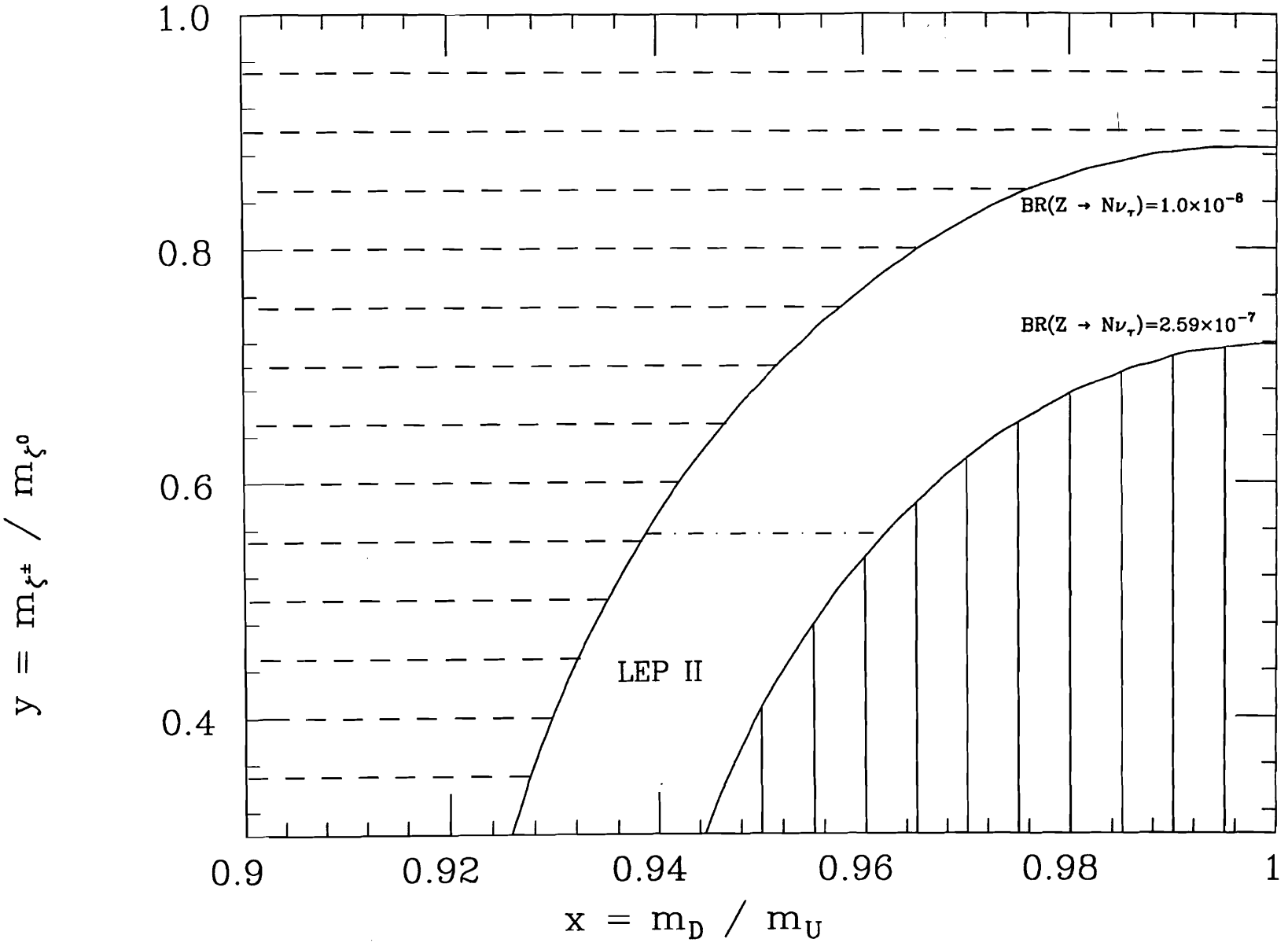
1.0
0.8
0.6
0.4
0.9
0.92
0.94
0.96
0.98
1
$y = m_{\zeta^\pm} / m_{\zeta^0}$
$x = m_D / m_U$
$BR(Z \to N\nu_\tau)=1.0\times10^{-8}$
$BR(Z \to N\nu_\tau)=2.59\times10^{-7}$
LEP II

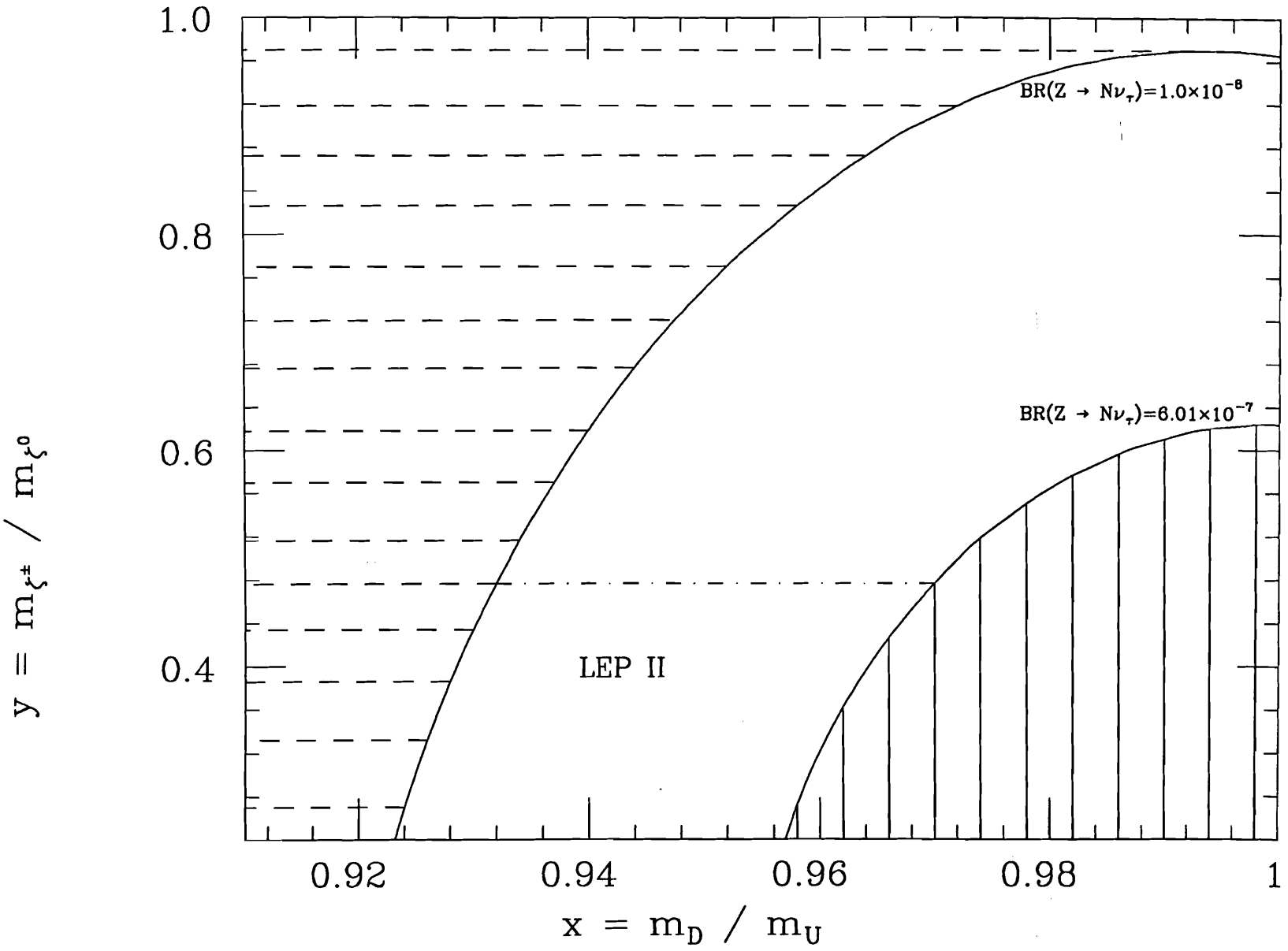
1.0
0.8
0.6
0.4
0.92
0.94
0.96
0.98
1
$y = m_{\zeta^\pm} / m_{\zeta^0}$
$x = m_D / m_U$
$BR(Z \to N\nu_\tau)=1.0\times10^{-8}$
$BR(Z \to N\nu_\tau)=6.01\times10^{-7}$
LEP II

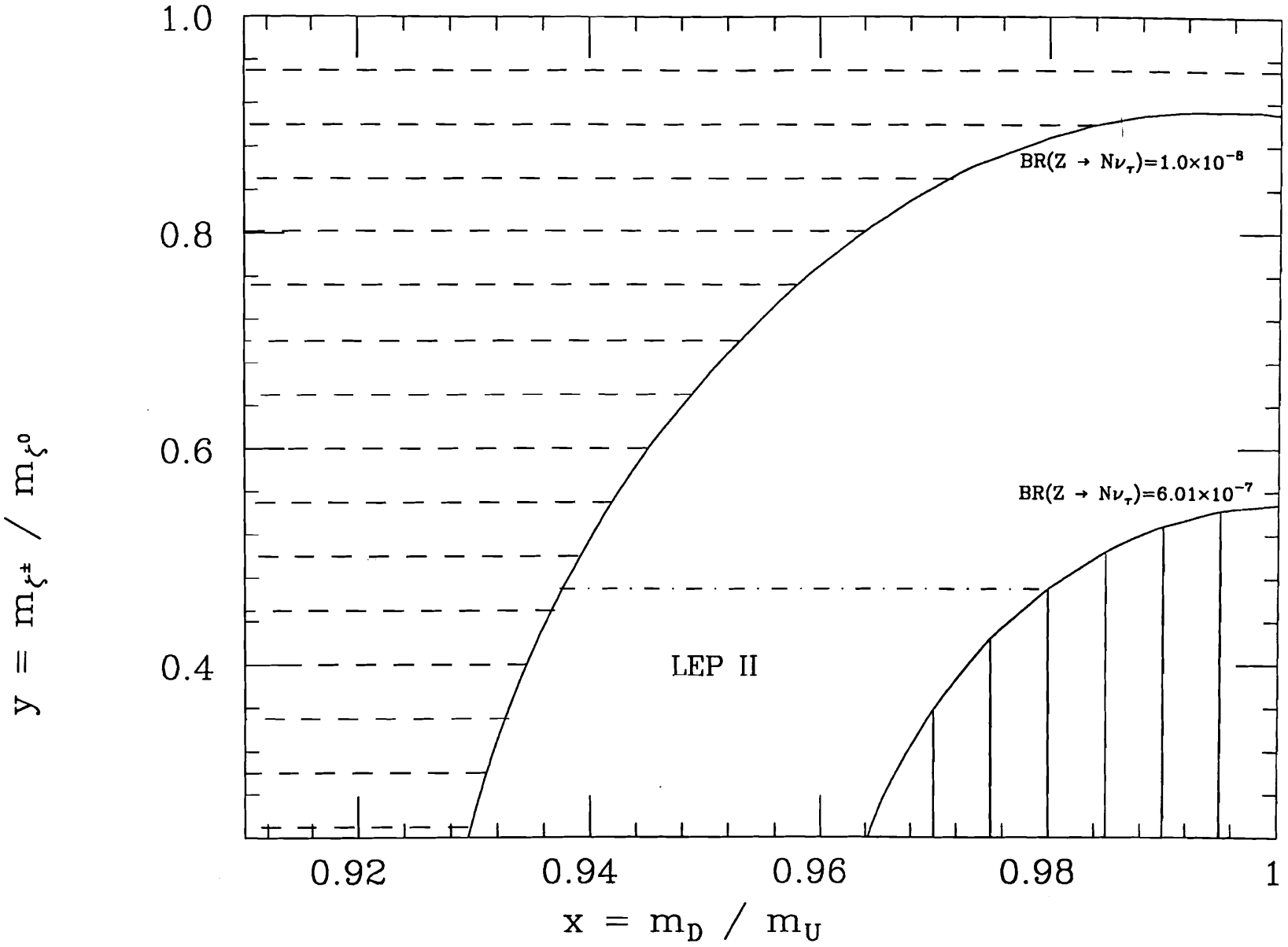
1.0
0.8
0.6
0.4
0.92
0.94
0.96
0.98
1
$y = m_{\zeta^\pm} / m_{\zeta^0}$
$x = m_D / m_U$
$BR(Z \to N\nu_\tau)=1.0\times10^{-8}$
$BR(Z \to N\nu_\tau)=6.01\times10^{-7}$
LEP II

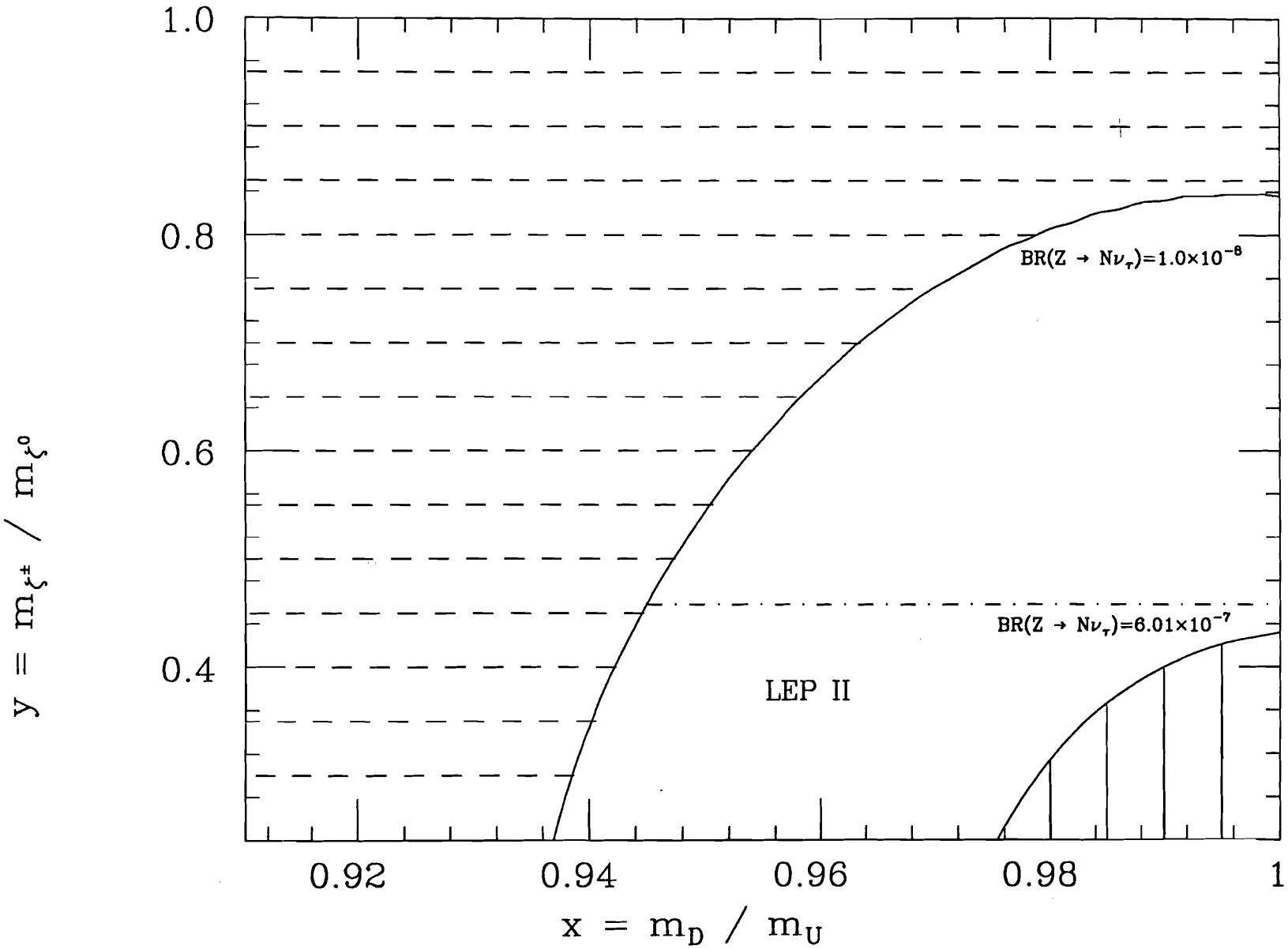
1.0
0.8
0.6
0.4
0.92
0.94
0.96
0.98
1
$y = m_{\zeta^{\pm}} / m_{\zeta^0}$
$x = m_D / m_U$
BR(Z → Nν$_\tau$)=1.0×10^{-8}
BR(Z → Nν$_\tau$)=6.01×10^{-7}
LEP II

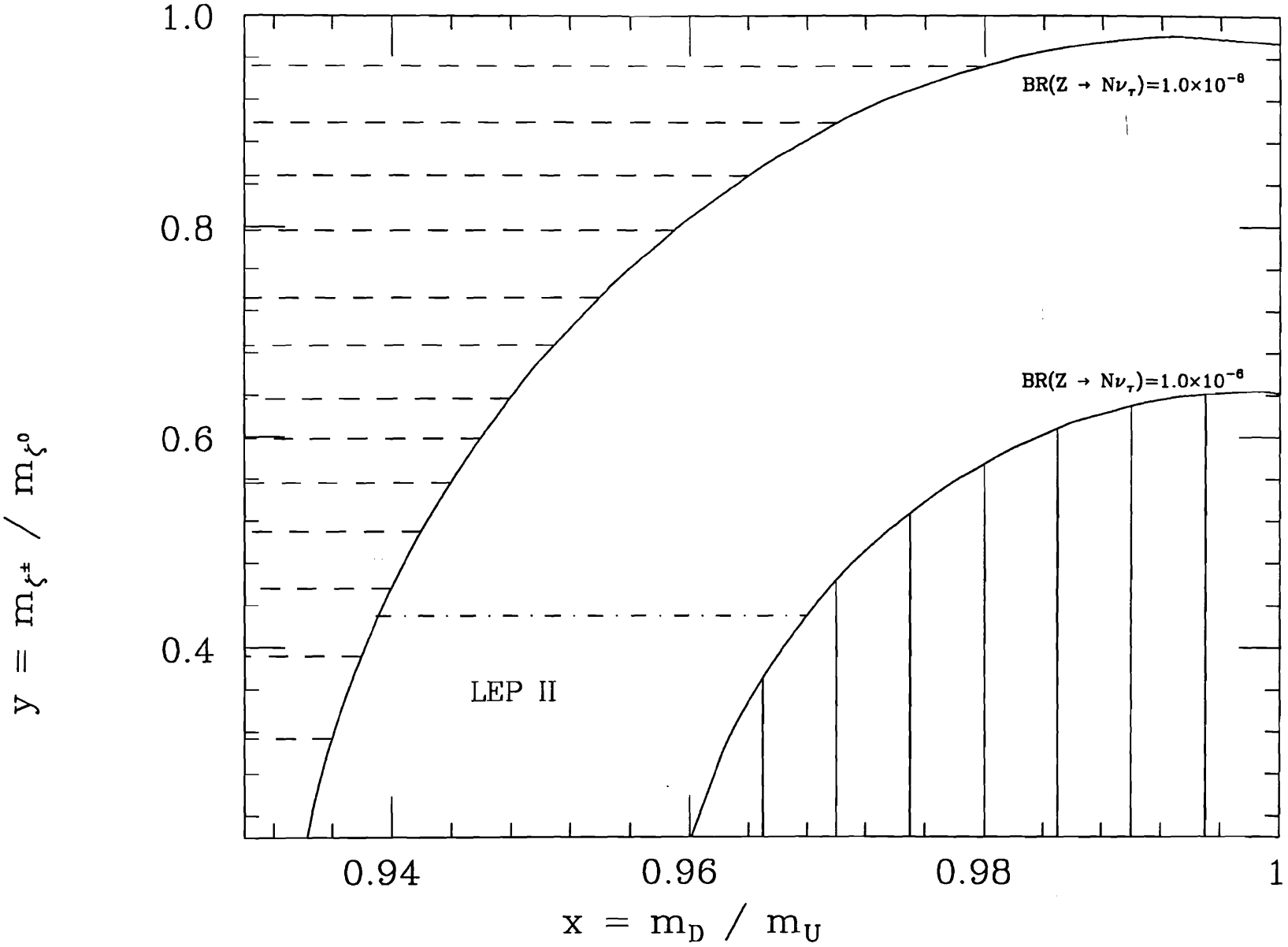
1.0
0.8
0.6
0.4
0.94
0.96
0.98
1
$y = m_{\zeta^\pm} / m_{\zeta^0}$
$x = m_D / m_U$
$BR(Z \to N\nu_\tau)=1.0\times10^{-8}$
$BR(Z \to N\nu_\tau)=1.0\times10^{-6}$
LEP II

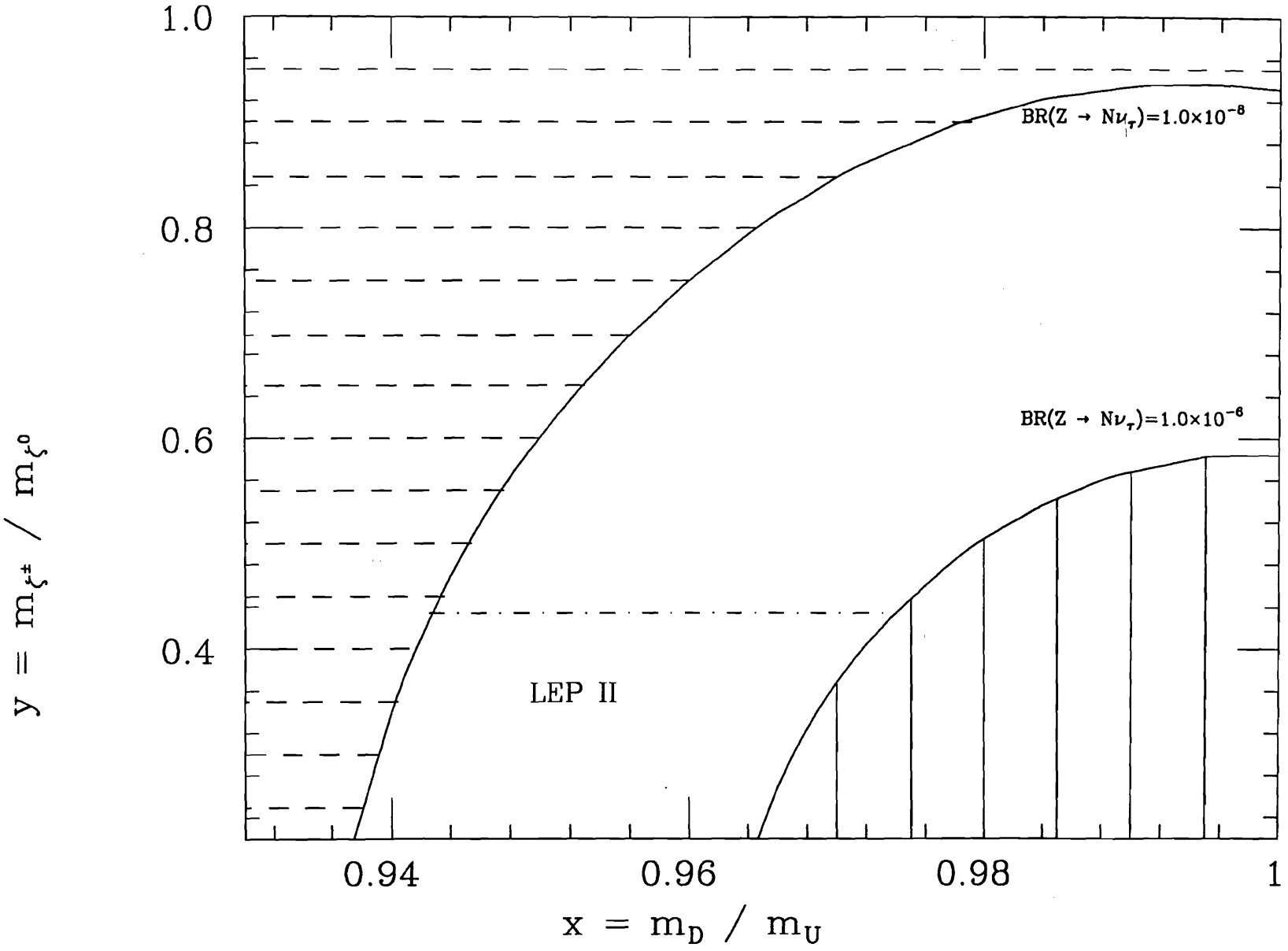
1.0
0.8
0.6
0.4
0.94
0.96
0.98
1
$y = m_{\zeta^\pm} / m_{\zeta^0}$
$x = m_D / m_U$
$BR(Z \to N\nu_\tau)=1.0\times10^{-8}$
$BR(Z \to N\nu_\tau)=1.0\times10^{-6}$
LEP II

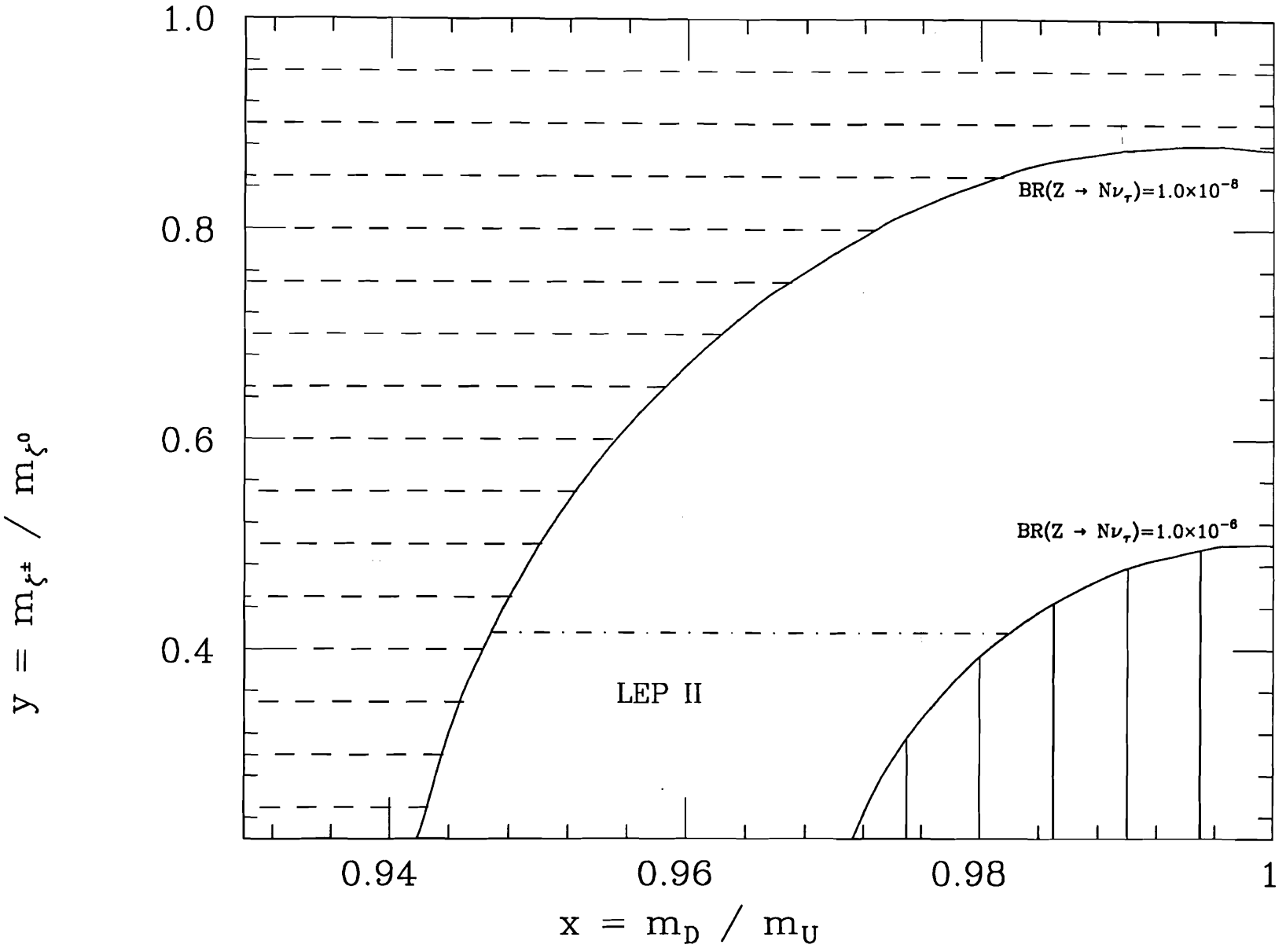
1.0
0.8
0.6
0.4
0.94
0.96
0.98
1
$y = m_{\zeta^\pm} / m_{\zeta^0}$
$x = m_D / m_U$
$BR(Z \to N\nu_\tau)=1.0\times10^{-8}$
$BR(Z \to N\nu_\tau)=1.0\times10^{-6}$
LEP II

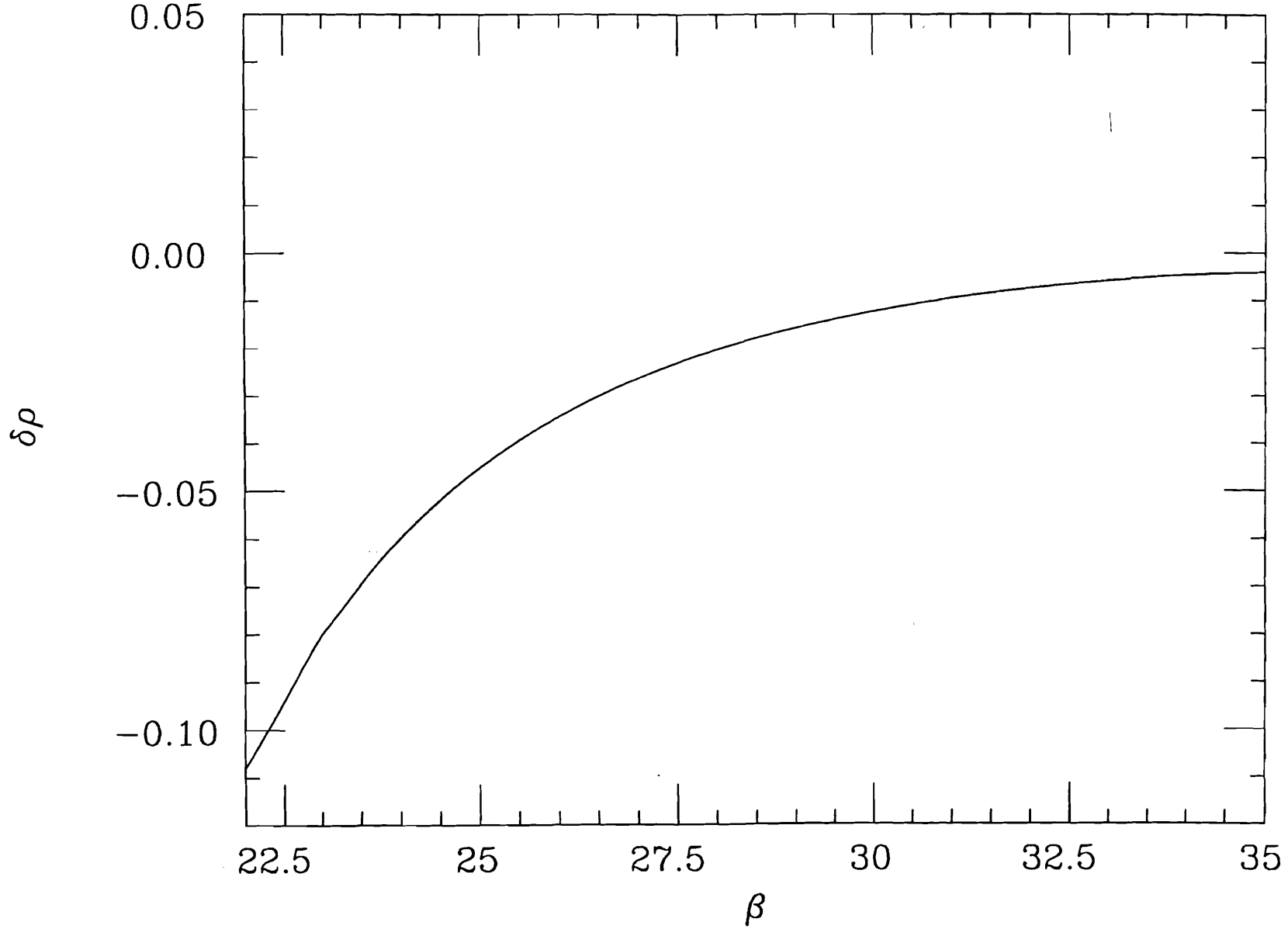
0.05
0.00
−0.05
−0.10
δρ
22.5
25
27.5
30
32.5
35
β

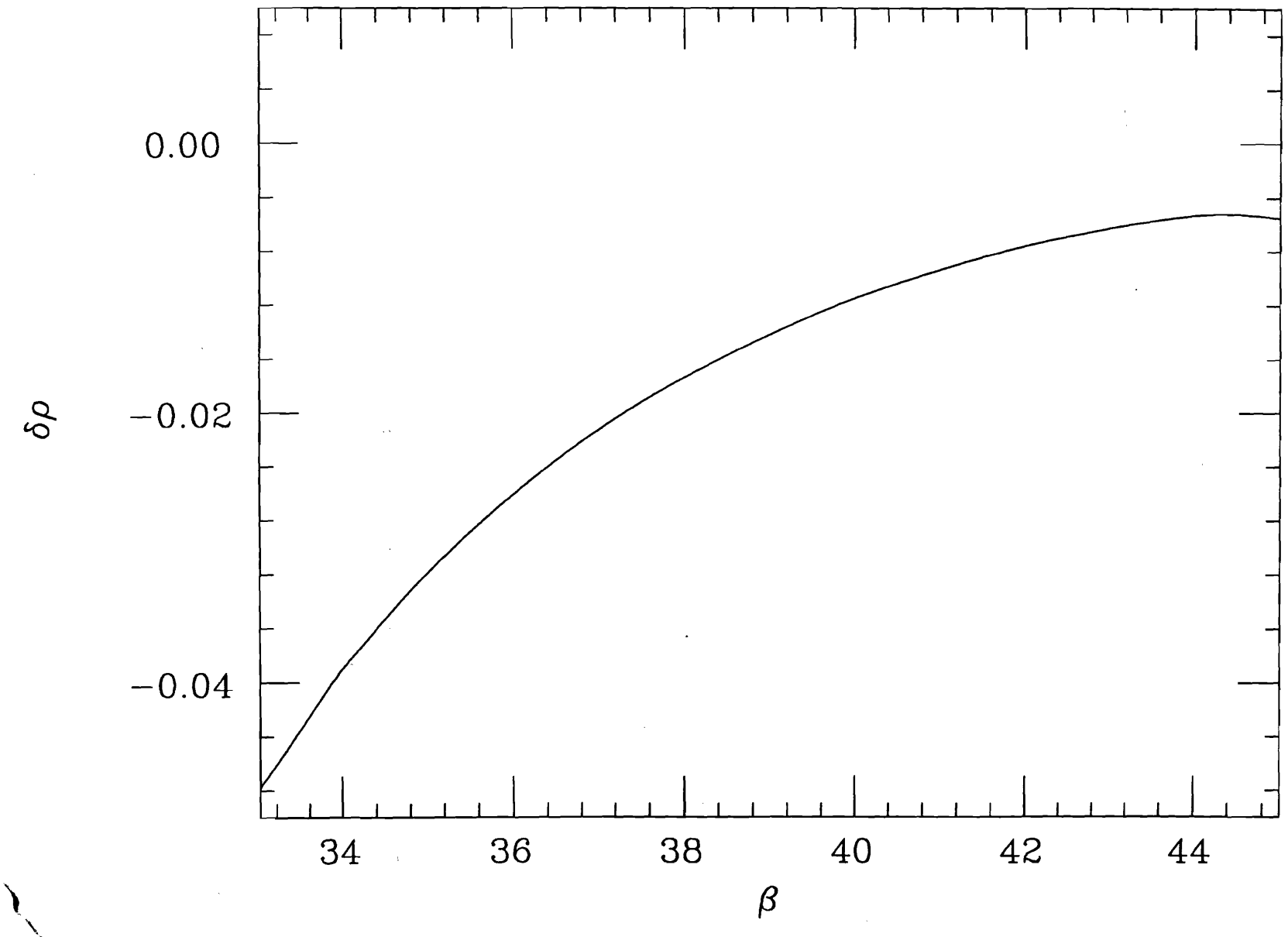
0.00
−0.02
−0.04
δρ
34
36
38
40
42
44
β